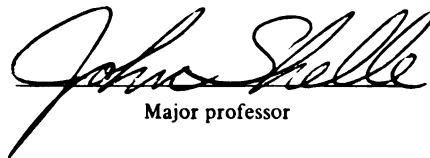This is to certify that the

thesis entitled

THE APPLICATION OF THREE-DIMENSIONAL
KINEMATIC METHODOLOGY TO THE EQUINE KNEE
AND ANKLE JOINTS

presented by

Camie Renee Heleski

has been accepted towards fulfillment
of the requirements for

Master of Science degree in Animal Science

Major professor

Date January 28, 1992

O-7639

PLACE IN RETURN BOX to remove this checkout from your record.
TO AVOID FINES return on or before date due.

DATE DUE	DATE DUE	DATE DUE
————	————	————
————	————	————
————	————	————
————	————	————
————	————	————
————	————	————
————	————	————

MSU Is An Affirmative Action/Equal Opportunity Institution

c:\circ\datedue.pm3-p.1

THE APPLICATION OF THREE-DIMENSIONAL
KINEMATIC METHODOLOGY TO THE EQUINE KNEE
AND ANKLE JOINTS

By

Camie Renee Heleski

A THESIS

Submitted to
Michigan State University
in partial fulfillment of the requirements
for the degree of

MASTER OF SCIENCE

Department of Animal Science

1991

ABSTRACT

THE APPLICATION OF THREE-DIMENSIONAL KINEMATIC METHODOLOGY TO THE EQUINE KNEE AND ANKLE JOINTS

By

Camie Renee Heleski

Three-dimensional videography and computer modelling were used to analyze flexion/extension, abduction/adduction, and internal/external rotation of the equine knee and ankle. The left knee and ankle of two "normal" (non-pathological) Arabian fillies were analyzed and evaluated during standing, walking, and trotting. Methodology similar to that used in human studies was applied. The forearm, cannon, and pastern were modelled as rigid bodies. Three, non-collinear targets were positioned on each rigid body. Four video cameras were set up in an arc around the level treadmill upon which the subjects were filmed. A previously written motion analysis computer package was used to analyze the data. Joint coordinate analysis programs were adapted from human research. After the data were plotted, curve shapes were compared and found to be similar from trial to trial within each horse. Basic curve shapes were similar, but differed in magnitude, between the subjects.

ACKNOWLEDGEMENTS

First, I would like to thank my graduate committee: Dr. Duane Ullrey, Dr. Robert Soutas-Little, and Dr. Ted Ferris, for their patience, support, and assistance in completing this project. They believed in me and gave me very helpful advice.

A special thank you to my major professor, Dr. John Shelle. His friendship, support, and willingness to tread new ground were greatly appreciated, as were the hours he spent shaping my thinking and reasoning skills.

I am eternally grateful to Dr. Soutas-Little, Dr. Charlie DeCamp, and the entire staff of the Human and Veterinary Biomechanics Evaluation Laboratories. These people all went above and beyond the call of duty to assist me with my project and to share their technology.

I am also indebted to Dr. John Stick for allowing me to use the treadmill at the Equine Performance Center and providing one of his technicians, Troy Trumbul, for the test date. In addition, Paula Fulkerson and her staff at the Horse Teaching and Research Center were instrumental in assisting me with the horses.

A blanket thanks goes to my office-mates and all the other graduate students, faculty, and staff who helped inspire

me, teach me, and provide friendship during my master's program.

Finally, I would like to extend grateful acknowledgement to my husband, Ernie, my family, and God for giving me the moral stamina to complete this endeavor. I would not be at this point without them.

TABLE OF CONTENTS

LIST OF TABLES

LIST OF FIGURES

INTRODUCTION

Despite a historic interest in analyzing equine locomotion, studies of which date back to the 1600's (Leach and Dagg, 1983a), there is a paucity of scientific literature to substantiate hypotheses concerning equine gait. In view of the potential applications for biomechanics in the growing horse industry, this lack of documented research is disturbing. Potential applications range from more accurate lameness diagnosis, to more appropriate corrective shoeing methods, from selecting athletes of the highest potential, to optimizing racetrack conditions (Leach and Dagg, 1983b).

Three-dimensional analyses have rapidly expanded the study of human biomechanics (Ulibarri et al., 1987). In light of this expansion, there is much potential for the impact three-dimensional analyses may have on explicating equine gait.

Due to the perceived need for more accurate information about equine gait analysis, this pilot study was undertaken to develop the methodology for three-dimensional kinematic data collection and analysis of the knee and ankle. This study was concerned with examining the flexion/extension, abduction/adduction, and internal/external rotation patterns which occur in the horse's knee and ankle. Three-dimensional data derived from high speed video films and analyzed using

1

joint coordinate analysis provided more complete information than have previous two-dimensional analyses, which have typically examined only the sagittal plane of motion.

The primary purpose of this study was not to establish a statistically significant base of knowledge of what "normal" knee and ankle kinematics are, but, rather, to develop a workable three-dimensional methodology to lay the foundation for future equine kinematic studies. It is hoped that after more work is done in identifying "normal" kinematic patterns in the knee and ankle, that work will proceed on more clearly identifying elusive lamenesses. Hopefully, studies will also commence on evaluating the effects of corrective trimming and shoeing. Similar methodology to that used in this study should also be applicable to other joints of the horse's body, such as the hock and stifle.

REVIEW OF LITERATURE

The study of biomechanics has appealed to researchers for centuries. Aristotle made general observations of locomotion patterns in quadrupeds during the Fourth Century B.C. (Smith and Ross, 1910). The first documented research of mechanics being applied to a living system was performed by Borelli (1608 - 1679), who worked on determining the center of gravity (Leach and Dagg, 1983b). Other research on quadruped locomotion by researchers such as Barclay (1953), Gray (1944, 1968) and Manter (1938) established the foundation upon which many equine studies were based.

One of the first documented studies of equine gait was performed by Newcastle in 1657 (Leach and Dagg, 1983a). Newcastle made detailed, though crude, descriptions of various equine gait patterns by listening to the sounds of hoof strike. During the 1700's, Goiffon and Vincent made careful records of equine locomotion patterns by attaching bells of different tones to horses' legs (Leach and Dagg, 1983a). In the 1800's, Lenoble du Teil (1877a and b, 1893), Goubaux and Barrier (1884) all made important contributions to the study of equine gait. They established the following understanding of horse gait: successive strides were quite similar; locomotion occurred in a cyclical manner; gait could be broken into stance/support and swing phases; and there were both symmetrical and asymmetrical gaits performed, such as the trot and the canter, respectively (Leach and Dagg, 1983a).

Professor E. Marey of France was one of the major contributors to early equine locomotion research. In the 1870's he developed a pneumatic automatic recorder, which was an india rubber ball filled with horsehair. He attached it to horses' hooves, and as they landed, changes in the balls' shapes would be registered. Secondly, he invented an india rubber box which fastened to the leg just above the ankle joint. As the leg moved, pressure was exerted on the box, which then moved a lever to record the movement on paper. His third invention was a set of two collapsible drums to which levers were attached to record vertical movements. These drums were fastened to the horses' croup and withers. For

faster gaits, he developed a device which the rider could hold between his teeth. Through these devices, Marey was able to determine precise sequences of hoof contacts. His calculations for the length of stance phase, however, were excessive (Leach and Dagg, 1983a).

The most important early contributor to the study of equine gait, as well as the "father of cinematography," was Eadweard (sic) Muybridge of the United States. In his primary work Animal Locomotion (1899), there are nearly 800 plates of animals, primarily horses, performing a multitude of gaits and maneuvers. Rumors abound regarding Muybridge's colorful entrance into the field of cinematography (Leach and Dagg, 1983a; Muybridge, 1899; Ulibarri, 1984). Supposedly, he was hired in the mid-1800's to settle an expensive bet ($25,000) made by Leland Stanford, financial founder of Stanford University. Stanford wanted to prove that all of a horse's hooves are simultaneously off the ground during a run. He also wanted his theory proven using his favorite race horse Occident. To perform the task, Muybridge first devised a camera with an exposure rate of 1/500 second. Unfortunately, the film of that era was not up to the task, and the first photos of Occident appeared as mere silhouettes. This led many people to question their authenticity. In 1877, Muybridge developed a camera with an exposure rate of 1/1000 second. These photos, though, were retouched, as was typical of that era, and again their authenticity was questioned.

Next, Muybridge set up a battery of 12 cameras alongside

a racetrack. Each camera was tripped when a horse ran by it. In 1878, in California, a horse named Sallie Gardner raced by the cameras. This set of photographs successfully showed the horse to have four hooves simultaneously off the ground during certain phases of the run. Muybridge was inspired and decided to create an atlas of movement for use by artists, his work Animal Locomotion. Soon after, he developed a projecting device, his zoogyroscope, which projected his sequences of photographs onto a screen. This was considered the forerunner of today's cinecamera (Leach and Dagg, 1983a; Muybridge, 1899; Ulibarri, 1984).

Today, though studies have not progressed as rapidly as one might have expected, the technology available for studying equine biomechanics has advanced tremendously. High-speed cine cameras today are capable of filming up to 5,000,000 frames per second (as would be used in a ballistics study) (Ulibarri, 1984). Within the last decade, technology for cinematography and videography in three dimensions has become available, however its use in horses thus far has been limited by cost and available facilities.

Other methods available for studying equine kinematics include accelerometers and electrogoniometers. Accelerometers are small, lightweight devices which attach to a body part to measure its acceleration. They are relatively inexpensive and both angular velocity and position values can be calculated (Leach, 1987). Electrogoniometers, or elgons, are devices positioned at the axis of rotation for a particular joint.

While they are relatively inexpensive and can be used for two-dimensional, as well as three-dimensional data collection, they have shown the following disadvantages in human studies: they restrict normal movement, add weight, and are difficult to secure precisely at the axis of rotation (Leach, 1987).

Force plates, force shoes, and pedobarographs are used to analyze equine kinetics. Again, while the technology is now available for three-dimensional analyses, its use has been limited in equines. A typical force plate would be a rectangular sheet of hardened aluminum with strain gauges or piezoelectric quartz transducers placed at each corner. When a limb strikes the plate, an electric charge proportional to the force applied is induced, amplified, filtered, and then stored (Leach, 1987). Force plates can measure a wide range of magnitudes. They can measure forces as small as those generated by a standing animal's heartbeat, to forces greater than a ton, which might be associated with a galloping horse (Pratt and O'Connor, 1976). Since sensitivity decreases toward the edges and corners of force plates, many attempts to achieve hoof strike in the center of the plate are often needed (Steiss et al., 1982).

Björck (1958) used horseshoes with strain gauges built into them to measure horizontal and vertical forces between the hoof and ground. Frederick and Henderson (1970) also developed a type of force horseshoe, but this device only measured vertical forces. A problem with both of these shoes was the additional weight they added to the hooves. In 1985

Ratzlaff et al. reported success with a lighter weight force shoe that measured vertical forces at the walk, trot, and canter. A ceramic piezoelectric disk was braced over the frog by struts attached to a racing plate. A cable from the transducer was attached to the leg and connected to a digital integrator which converted the output to a voltage proportional to the force. Force shoes may become preferable to force plates since they can be used to measure successive strides, and the problem normally encountered with subjects trying to bypass the force plate is avoided (Ratzlaff, 1985).

A system utilized by the Scottish Farm Buildings Investigation Unit is the pedobarograph. This system simultaneously measures the distribution of pressure on the limb and the three-dimensional force pattern of the limb kinetics (Leach, 1987). Thus far, it has been used primarily for cattle and pigs.

The following examples demonstrate how kinetic studies might be useful. Björck (1958) found that when draft horses pulled a load, the hind limbs contributed a larger horizontal force than they did when the animals were unloaded. Dalin and Fredricson (1972) showed that the maximum vertical force in the forehoof of a trotter was about 8000N (Newtons). Schryver et al. (1978) found that peak vertical forces for the walk were equivalent to 60% of bodyweight. Peak vertical forces at the trot were found to be 90 - 100% of bodyweight (Quddus et al., 1978; Schryver et al., 1978). While studying Standardbreds and Thoroughbreds, Rooney et al. (1978) found

peak vertical forces at the gallop to be 175% of bodyweight.
Work by the aforementioned researchers, as well as Bartel et
al. (1978), Geary (1975), and Pratt and O'Connor (1976), has
shown that the limb (during stance phase) generates a
horizontal decelerating force and then after the peak vertical
force, generates an accelerating force. The decelerating or
restraint phase is slightly longer in the hind limbs than the
fore limbs, but in both sets lasts about 40 - 45% of the
stance phase. Also, horizontal force is minimal at toe off;
i.e. when the toe of the hoof leaves the ground.

Auer et al. (1980) and Gingerich et al. (1979, 1981) used
force plates to evaluate improvement or regression in the
weightbearing ability of horses with osteoarthritis of the
knee. Rybicki et al. (1977) demonstrated that the forces
occurring in the tibia and metacarpus while an animal
struggles to rise after being anaesthetized are greater than
those forces recorded during the trot.

A Japanese group headed by Yoko Niki has done several
studies using force plates. In 1982 they demonstrated a
difference between the walk and trot in that the walk shows
two vertical force peaks in both front and hind limbs, while
the trot shows only one peak. At the walk, they determined
peak vertical values in the front legs to be 56.2 - 68% of
bodyweight and in the hind legs to be 42.9 - 48.6% of
bodyweight. At the trot, peak vertical values registered as
105% of bodyweight in the front legs, and 92.8% of bodyweight
in the hind legs. These results lend support to the commonly

held theory that the fore legs provide the function of support, and the hind legs provide the function of propulsion (Ueda et al., 1981).

Merkens and Schamhardt (1988) demonstrated that in clinically sound horses the distribution of ground reaction forces in concurrently loaded limbs was quite similar; i.e. there was nearly complete symmetry between both the forelimbs and the hindlimbs. Upon testing a lame horse, they found the ground reaction forces to be significantly lowered in the lame leg, but significantly greater in the other three limbs. Their studies have used the Dutch Warmblood horse as their subject. They have recently developed the H(orse) INDEX to quantify and classify horses based on ground reaction force patterns. This standardized index combines limb and symmetry indices. Force plate measurements from pathological horses are compared to graphs of over 20 "standard" Dutch Warmbloods, which are on file. This has helped them classify locomotor performance.

Preuschoft (1989) found that due to a horse's ability to distribute load over all four limbs during take off and landing for jumps, these stresses often did not exceed those obtained during fast dressage gaits. However, he showed that if the distal limb segments are not placed perfectly parallel to the external force's direction, the torque may exceed the tissue strength of bone, causing breakage.

Before equine kinetics, which is the study of forces, can be completely understood, knowledge of the center of gravity

and moments of inertia of body segments must be obtained (Sprigings and Leach, 1986). Frontal plane center of gravity for the whole body of standing horses has been found by Benke (1934), Krüger (1940, 1941), Rettenmaier (1950), and Björck (1958). Though the computation of changing centers of gravity during movement had been attempted,(Hayes, 1893; Chieffi and de Mello, 1939; Hékimian, 1970), until recently such computations were incomplete and inaccurate.

In 1986 Sprigings and Leach used Thoroughbred-type horses to: 1) establish a standard method for disarticulating equine cadavers for the purpose of determining centers of gravity, 2) demonstrate a technique for locating centers of gravity in two dimensions, and 3) present the algorithm required to use segmental data to determine whole body center of gravity from cine film analysis.

Using kinematic methods (those methods which evaluate motion), researchers have discovered that horses will make preferential use of certain limbs during exercise; i.e. "handedness" can be observed (Bayer, 1973; Drevemo et al., 1980a; Drevemo et al., 1980b; and Howell, 1944). Drevemo's group determined that racing trotters often showed a preference for using particular limbs or a particular diagonal pair. Using high-speed cinematography, Deuel and Lawrence (1985b) observed bilateral asymmetry in the gallop of Quarter Horse fillies. Given equal opportunity for choosing each lead, these horses chose the left lead nearly twice as often as the right, and often switched to the left lead even if they

started on the right lead. The researchers theorized that the right trailing limb would be able to withstand greater stresses. This laterality may actually play a part in influencing athletic performances, particularly when one examines data that show some horses race more successfully in the United States than in Europe and vice versa. (Races are run counter-clockwise in the United States and, typically, clockwise in Europe.) Since human subjects tend to be stronger, faster, and more accurate on the same side of their body as the hand they write with (Borod et al., 1984), these findings on "horse handedness" are not unexpected.

Numerous studies have been performed researching the relationships between speed, stride length, and stride frequency (Dalin and Jeffcott, 1985; Drevemo et al., 1980a; Leach et al., 1987; Rooney, 1984; and Schryver et al., 1978). Many performance events, such as dressage, are based on a qualitative evaluation of these relationships as they relate to a particular judge's opinion of the ideal "way of going."

Stride length multiplied by stride frequency gives velocity. Deuel and Lawrence (1985a) showed that both stride length and stride frequency increased with increasing velocity, at least at the gallop. Dusek et al. (1970) showed that when speeds were greater than 12 m/sec, velocity increases were due mainly to increased stride frequency. Using Standardbred trotters, Drevemo et al. (1980a) showed that the mean stride length was 545 cm and the mean stride duration was 455 milliseconds. The hind limbs had a longer

restraint period than the front limbs, resulting in slightly shorter swing phases in the hind limbs. In a separate study, Drevemo et al. (1980c) demonstrated that the variations in a particular horse for stride length, stride duration, stance time, swing time and propulsion time were very small. There was somewhat more variation in the restraint stage. Due to the close correlation Drevemo's group found between stride and swing phase duration, it appeared that swing phase was the main contributor to stride-time variation among horses trotting. Their findings led them to believe that an analysis of 3 to 5 strides should be adequate to gain an understanding of a particular horse's stride. Drevemo et al. (1980a, 1980b) and Fredricson et al. (1972) have shown very stable patterns of repeatability when analyzing ten or more strides from Standardbred trotters.

Schryver et al. (1978) found that motion for the digit is very similar at the walk and the trot. Angular velocities, however, increased as the speed of the horse increased and the support time decreased. The minimum value for the pastern angle was also found to be less at the trot than at the walk; i.e., the ankle joint sinks lower during the trot.

Rooney (1984) compiled a table showing various researchers' results on stride frequencies, lengths, and velocities for several gaits. Data for the walk showed frequencies of 0.84 and 1.05 strides/sec, velocities of 1.26 and 2.26 m/sec, and stride lengths of 1.5 and 2.15 meters (Muybridge, 1899). Muybridge found the trot to have a stride

frequency of 1.54 strides/sec, the velocity to be 6.34 m/sec, and the length to be 4.12 meters. Rooney found the racing trot to have a frequency of 2.27 strides/sec, a velocity of 13.42 m/sec, and a length of 5.9 meters. Values for the canter/gallop ranged from a frequency of 1.33 to 2.32 strides/sec, velocities of 4.59 to 17.12 m/sec, and stride lengths of 3.45 to 7.38 meters (d'Enrödy, 1967; Pratt and O'Connor, 1978). When Rooney made curve fittings of these data, he found that velocity to stride length had a correlation coefficient of 0.95. Velocity to stride frequency had a correlation coefficient of 0.84, and stride length to stride frequency had a correlation coefficient of 0.64.

In one of the few kinematic studies large enough to use multivariate statistics, Leach et al. (1987) analyzed 17 stride-timing measurements of 22 racing Thoroughbreds. The horses were filmed at the beginning of races, while performing right-lead transverse gallops; i.e., the diagonal pairs were working together. Mean stride duration was found to be 0.405 sec and mean stride frequency was 2.47 strides/sec. From their research, they predicted that diagonal limbs should act more synchronously and that the overlap between the lead hind limb and nonlead forelimb would decrease as velocity increased. It appeared that at faster velocities, these subjects would tend to "rabbit-hop" by using their hind limbs more in synchrony and by dissociating the action of these limbs from the action of the forelimbs. This type of locomotion would appear to rely more heavily on back

flexibility.

Deuel and Lawrence (1988) studied neck and shoulder motion of the gallop stride. Many differences were noted between the body's leading and trailing sides; e.g. the minimum and maximum heights of the scapula, which differed from side to side. The work needed to vertically displace the center of mass while galloping was estimated to be 98,500 J/km, which approximates 6% of the total energy expenditure for 1 km.

Work performed by Deuel and Park (1989) at the 1988 Olympics provided the first quantitative documentation of temporal patterns in Grand Prix-level dressage horses. These researchers found positive correlations among forelimb impact intervals, swing phase durations and the judges' scores. Another study done on performance horses examined cutting horses (Clayton, 1988). Clayton found that the highly successful performers had faster reaction times and positioned their body more closely, and more nearly head-on to the cow. One study which looked into the rider's effect on horse performance examined the effects of urging by jockeys (Deuel and Lawrence, 1988). Their cinematographic study showed that whipping the horse on the shoulder once per stride (typical urging) did not increase the average velocity of 12.6 m/sec, although it did increase stride frequency while decreasing stride length.

One of the greatest potential applications of applied biomechanics lies in diagnosing lamenesses. Estimates

indicate that over 500 million dollars are lost to lameness annually in the U.S. Thoroughbred industry alone (Mackay-Smith, 1977). Losses consist of lost racing days, reduced performance, salvage costs associated with lameness, reduction in value of lame horses, and decreased betting due to small fields (Leach and Crawford, 1983).

In one study of lameness, May and Wyn-Jones (1987) placed markers on each tuber coxae to help identify relative movement of the hindlimbs at the trot. During hindleg lamenesses, the tuber coxae on the lame side showed an increase in vertical displacement compared to the other limb. Ratzlaff et al. (1982) used kinematic methods to define the movements of the carpal joints and attempted to correlate these with lamenesses. One example of what this group found was that a horse with a swinging leg lameness (i.e., lameness observed while the leg is in flight) of the right limb showed decreased flexion, increased support time, and decreased angular velocities compared to sound horses.

Using forceplates, Gingerich and Newcomb (1979) found that after inducing arthritis via a small intercarpal chip fracture, horses still carried nearly 60% of their weight on the forequarters, but dramatically shifted the weight off the arthritic limb to the limbs on the opposite side. When Ratzlaff et al. (1982) used electrogoniometers to evaluate carpal lamenesses, they found the lame horses had decreased flexions and irregular extension phases. Horses with swinging leg lamenesses showed decreased flexion and decreased angular

velocities during flexion. Horses with supporting leg lamenesses (lamenesses observed during stance phase) showed shortened periods of maximum extension during support and decreased angular velocities during the extension phase.

Leach (1987) stated that, "Many of the locomotion analysis techniques generate data which may be difficult to relate to a mental image of a moving horse. Decisions based on these data will, therefore, have to rely on results of statistical analysis. To refine such procedures, an adequate data base of sound horses and horses with known lamenesses must be available for comparison." He feels an integration of three-dimensional kinematic and kinetic data might ultimately provide an effective lameness evaluation system for horses.

To date, there have been few studies performed in which the effects of trimming and shoeing have been quantitatively monitored. If quantitative analyses were made of the kinetic and kinematic changes occurring after farrier modifications, and this information was combined with any observed pathologies or improvements, a clearer relationship could be made to approach a more objective type of farrier science.

Rooney (1984a) devised mathematical theories to prove that decreasing the hoof angle, i.e., to make it steeper with the ground causes elevation of the pastern, an increased palmar angle of the coffin joint and increased dorsal angle of the fetlock joint, an increased tension and strain of the deep flexor tendon, and a decreased tension and strain of the interosseous medius muscle with little or no change of the

superficial flexor tendon.

After studying the flight of the hoof via high-speed cinematography and computer-aided analysis, researchers at the University of Florida and the Western College of Veterinary Medicine (Kilby, 1988) have discovered that many commonly held theories about hoof flight do not hold true. The analyzed hoof flights were not as smooth nor as high in amplitude as the theoretical models. These researchers also found that most horses' hoof angles are steeper than commonly believed - averaging 53.5° in the front and 54.8° in the back, versus the theoretical 45° and 50° for the front and back, respectively. Since a wide range of angles was identified in sound horses, it was felt that any angle which corresponded to the horse's pastern angle was probably appropriate for that individual. Interestingly, the common practice of changing hoof angles to affect pastern angles was found to be an undesirable practice. Turner's group from the University of Florida found it took 10° of change in hoof angle to change the fetlock, or ankle, angle 1°. This change did, however, add significant stress to the pastern and coffin joints.

Along these same lines, Dr. Ric Redden, who operates the International Equine Podiatry Center in Kentucky, has also seen more joint problems in young horses with over-corrected limbs than with those trimmed in a balanced fashion; i.e., when the hooves are allowed to be of equal length on each side (Herbert, 1988).

When a foal is born with deviated (less than straight)

conformation, and is consequently correctively trimmed, Dr. Redden expressed a concern that the foal may place undesirable compressive loads on his unclosed joints. He says, "One reason excessive corrective trimming has gained popularity is due to the optical illusion that it gives to the limb." He has started collecting radiographs of the feet and ankles of foals he has seen. Thus far, he has found the degree of limb deviation has much less correlation with deformed ankles than the correlation between this problem and highly corrected legs. Redden does feel some correction can be beneficial if done in moderation. He defines correction as follows: "to take an individual with an angular limb deformity and correct him in such a manner that the correction improves his dynamic stability." He feels harsh corrections made on young horses primarily for cosmetic reasons often impairs the ability of the horse to carry his weight as an exercising adult. He explains that while splay legged horses (i.e., the entire leg is rotated outward) may never win a conformation class, when considering the stress alignment of the joints, these horses may have a minimal problem.

Unfortunately, there have been very few scientific studies done on shoeing and trimming. A great deal of open-minded empirical evidence supports the following: leave horses barefoot as long as possible, do minimal corrective trimming, do not use toe grabs on shoes, and do not trim for long toes and low heels - which is the common practice for trimming Thoroughbred race horses (Ivers, 1985).

Biomechanical analyses can also be used to evaluate the horse's competitive environment. Swedish researchers have looked at the effects of racetrack design on limb positioning of Standardbreds (Dalin et al., 1973; Fredricson et al., 1972; Fredricson and Nilsson, 1974; and Fredricson et al., 1975 a, b). Their work showed that the conventionally-shaped track with its constant turn radius is insufficiently banked to maximize performance longevity. The relatively sharp turns appear to contribute to excessive bone stress. Cheney et al. (1973) examined racetrack surfaces as they related to Thoroughbred lamenesses. Not surprisingly, they found that tracks with pliant, loose surfaces dramatically decreased the incidence of lamenesses.

Most of the previously mentioned works have consisted of two-dimensional studies. Published three-dimensional biomechanical studies are still very limited in the equine literature. Fredricson and Drevemo (1971) used a method, which had previously been used on aircraft, to analyze yaw, pitch, and roll (three dimensions) of the hoof via a glass-fiber molded shoe with coordinate markers. Unfortunately, this system was not functional for other joints and the weight of the shoe may have influenced movement. It did, however, emphasize the importance of analyzing all three dimensions of motion for certain types of studies, such as elusive lamenesses.

Recently, Peloso et al. (unpublished data, 1990) discovered that the human eye's slowness has contributed to

another myth. Using three-dimensional videography, he discovered that horses actually raise their heads when they land on the sound fore leg, not the lame fore leg as has been commonly believed.

Within the last decade there has been rapid expansion in three-dimensional motion analysis in humans. Ever since Grood and Suntay (1983) devised a method of applying rigid body mechanics to the knee, progress has been rapid. Shortly thereafter, a joint coordinate system was devised for the ankle (Soutas-Little, et al., 1987). Similar concepts, using different joint coordinate systems for various joints should be applicable to the horse.

MATERIALS AND METHODS

Two subjects were selected for this pilot study of three-dimensional kinematics in horses. The subjects were two-year-old Arabian fillies from the Michigan State University Horse Teaching and Research Center. Both fillies were considered "normal" (i.e. not pathological) in both conformational build and movement. To prepare the horses for the trial, the fillies were acclimated to the Horse Center's treadmill for one month prior to the experiment. The fillies were walked and trotted on the inclined treadmill three times per week. By the trial date, they accepted the treadmill workouts quietly.

One of the most important aspects of this trial was to set up an appropriate targeting scheme to detect three-

dimensional motion of the horse's knee (carpal) and ankle (metacarpo-phalangeal) joints. The targeting scheme which was developed is represented in Figure 1. Three-dimensional analysis requires that the biological system be modelled as though it were composed of rigid bodies. For this protocol, the forearm and cannon were the rigid bodies for the knee joint, and the cannon and the pastern were the rigid bodies for the ankle joint. Three, non-colinear points were necessary on each "rigid body" to facilitate later three-dimensional analysis. Two of these points had to be in line with an anatomical axis, and all three points had to lie in an anatomical plane. For the forearm targeting scheme, targets one and two were aligned with the radius of the left front leg. Targets four and five were placed just off the surface of the metacarpus, and targets seven and eight were aligned with the proximal and middle phalanges.

Fastening the targets to the horse to minimize target wobble and subject discomfort was difficult. There were several reasons why targets could not be placed directly on the horse's skin. At the forearm, there exists a fair quantity of muscle. This muscle moves over the bone and distorts the true joint motion. Another problem was that as the horses started to sweat, the targets were likely to fall off. Regarding the pastern, there was such a small amount of space to evaluate that it would have been difficult to place the targets directly on the pastern and have the cameras "see" them without distorting the target images into "mergers."
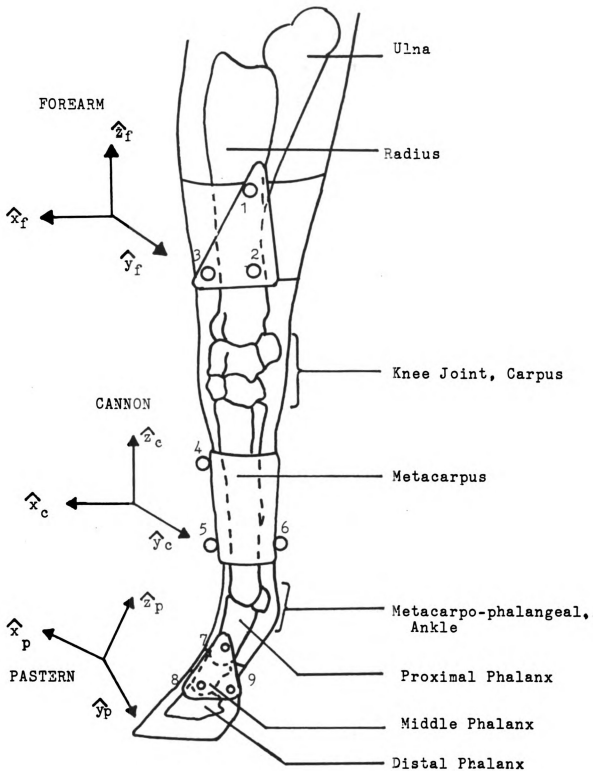
Figure 1. Lateral view of the left, lower leg showing targetting scheme and coordinate systems.

(Mergers occur when two targets are close enough to each other that, at certain angles, the cameras "see" two targets as one large target.) Targets were not placed on the hoof since there appears to be a great deal of movement between the middle and distal phalanges; consequently, this would not have represented an appropriate rigid body.

The forearm targeting scheme was set up in the following manner: first, a piece of thick leather was formed to the curvature of the horse's forearm, then a block of wood was cut to fit the curved leather and to raise a flat, triangular piece of leather from the horse's leg. The raised piece was parallel to the plane of the forearm. The three targets were positioned on this planar piece of leather with double sided carpet tape. Elasticized bandaging wrap was used to secure the target scheme securely to the subject's leg.

A standard splint boot (typically used on young horses' cannons to avoid injury) was securely tightened to the cannon. This was then wrapped with elasticized bandaging wrap. The targets were then stuck to the wrap with the carpet tape. First aid tape was then slit to go over the targets to further secure them. The pastern targeting scheme was similar to the forearm model, only smaller. A velcro band was used to secure the targeting scheme tightly to the pastern.

Targets were made with strips of retroreflective tape wrapped around spherical bases of different sizes. (It is the reflection from these targets that the cameras record as data.) Forearm targets were 2 cm in diameter; cannon targets

were 2.5 cm in diameter; and pastern targets were 1.5 cm in diameter. Targets were glued with epoxy to flat spheres of leatherette material. This flat base was then easier to stick to a targeting scheme platform than the spherical target itself.

Before the horses could be filmed, the volume of space in which the horse's leg would move had to be calibrated. The calibration structure consisted of 16 non-coplanar control points with known coordinates. It defined a control volume of 105 cm x 90 cm x 170 cm (see Figure 2). The four points on each of the four strings of the calibration jigs were located 15, 45, 75, and 105 cm above the treadmill. Great care was taken to ensure that the calibrated volume was as precise as possible. After all distances were carefully measured, the calibration structure was filmed to see how closely the measured volume compared to the filmed volume. After the first calibration setup, the residuals (determined by Least Squares technique- Walton, 1981) were as high as 0.7. It was discovered that the treadmill flooring floated up and down slightly. For the second attempt at calibration, the treadmill flooring was not touched while measuring the calibration points. The second set of residuals registered 0.55, 0.31, 0.40, and 0.57 for cameras one through four, respectively. Since easily tracked data had previously been collected with residuals of 0.6 and below, these values were deemed acceptable.

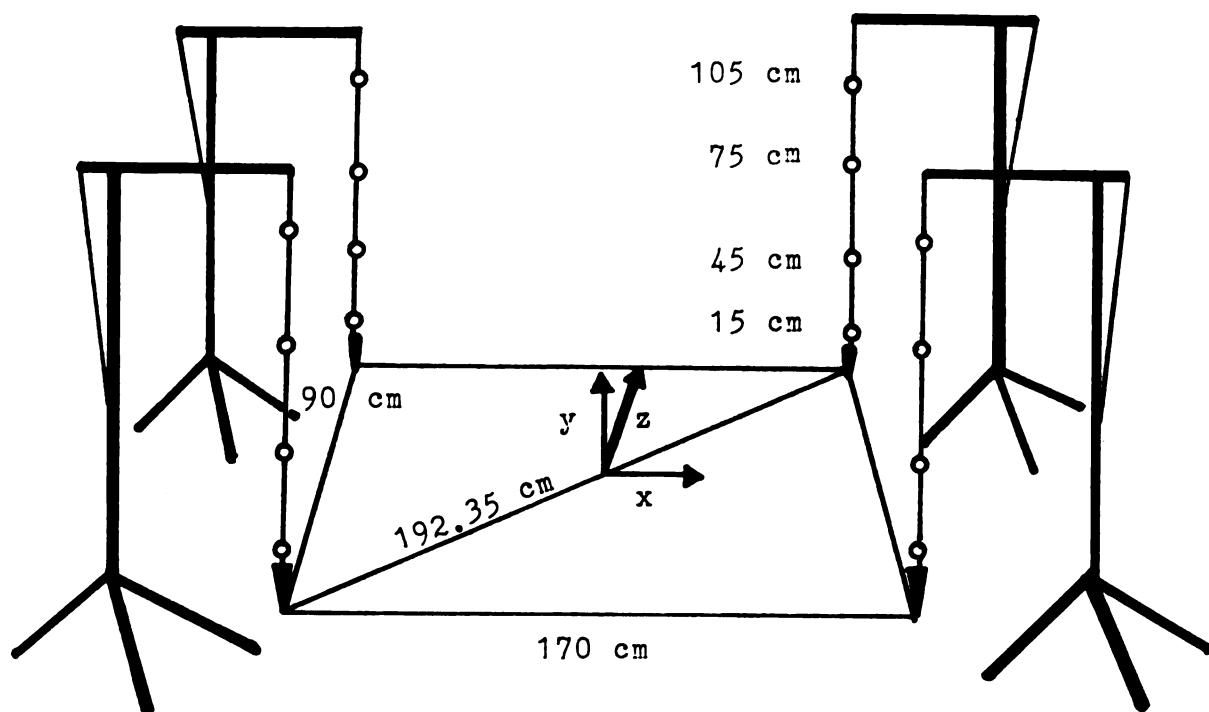Cameras were set up in a semi arc around the left side of

Figure 2. Calibration structure, showing calibrated volume and the sixteen coordinate points.

the treadmill in the MSU Equine Performance Center of the Veterinary Clinical Center. The video cameras were set at 60 Hz, meaning that they took 60 frames of data per second. Since each trial consisted of three seconds, 180 frames of data were collected per trial. Camera one was approximately 12 m from the calibrated space and positioned anterio-sagittally. Cameras two and three were located approximately 11 m from the calibrated volume and filmed sagittally. Camera four was approximately 12 m away and filmed posterio-sagittally (see Figure 3). If the residuals are acceptable, and all targets can be viewed by the cameras, precisely measured camera distances are not necessary. After the calibration structure was removed, the horses were acclimated to the treadmill. Since this treadmill was quieter and more open than the treadmill the fillies had been trained on, this was accomplished relatively easily. The horses were filmed at a standstill (to provide offset angles for later analysis), at the walk, and at the trot. Three trials of each gait for each subject were filmed and sent to the video processor (Motion Analysis VP320). The treadmill speeds selected were 1.6 m/sec and 3.5 m/sec for the walk and the trot, respectively.

After data collection was completed, data analysis could begin. A program known as EV3D (Expert Vision - Motion Analysis Corporation) was used to analyze the data. (Access to this program was generously provided by the Human and Veterinary Biomechanics Evaluation Laboratories). First, all data were copied to the SUN SPARC Station 1 (Sun Workstation -

Calibrated Space

Treadmill

Direction of Horse Movement
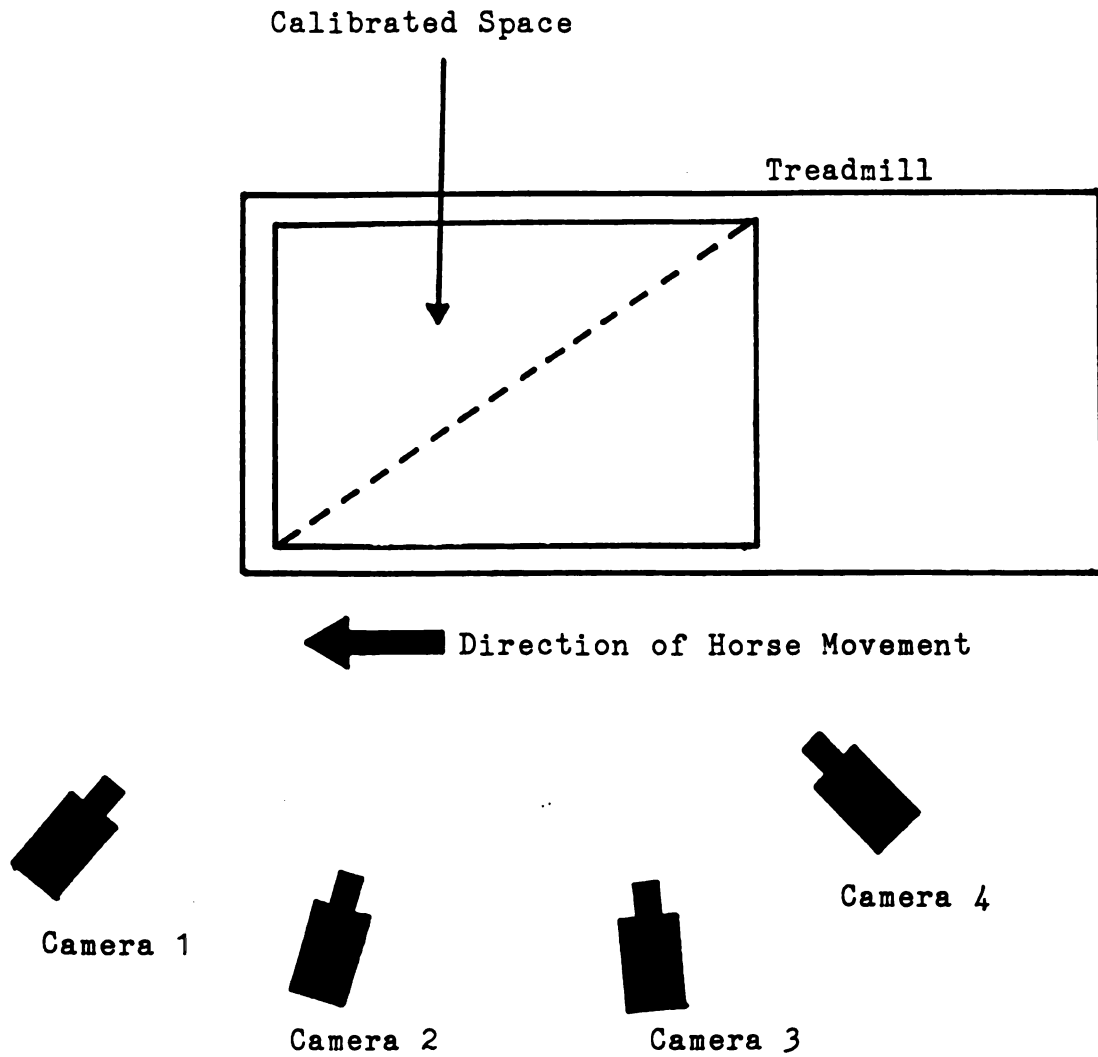
Camera 1

Camera 2

Camera 3

Camera 4

Figure 3. Overhead view of the calibrated space in relation to the treadmill, and the position of the cameras.

Sun Microsystems, Inc.) from the original data collection disks. The calibration files from each camera were entered and "tracked." The tracking procedure involved initializing the computer to the target numbers seen in each camera view. Each point was then "track edited" to ensure there were no obvious errors in the data. Environmental variables were entered into the program (see Table 1). Some of these values came from the calibrated space measurements; other values were selected based on the experiences of the MSU Human and Veterinary Biomechanic Laboratories. After this, the horse trials could be analyzed.

Each of the four cameras' files was first viewed to check for merger (see Figure 4). When this happened, the camera was interpreting two targets "merging" together. This phenomenon greatly reduces the accuracy of the analysis. Since mergers were not observed in the data from cameras two and three, but were frequently observed in cameras one and four, the latter two camera files were "masked." In the masking program, any observed mergers could be deleted from the data files. (This was a plausible alternative since only two cameras needed to "see" a target at a given time to allow three-dimensional interpretation.) Most typically, targets eight and nine would merge in camera views one and four, but, occasionally, other mergers were observed.

Next the masked files were tracked using the same procedure as for the calibration structure (see Figure 5). Targets were identified in a frame and then the program would,

TABLE 1

Environment

```
1       Segmentation Neighborhood Width (pixels)          2.00
2       Segmentation Neighborhood Height (pixels)         2.00
3       Minimum number pixels in image of single target   4.00
4       Maximum number of pixels in image of single target 25.00
5       Maximum norm of residuals (pixels)                .900
6       Min. X coordinate delimiting object space (cm)   -160.0
7       Max. X coordinate delimiting object space (cm)    160.0
8       Min. Y coordinate delimiting object space (cm)   -90.0
9       Max. Y coordinate delimiting object space (cm)    90.0
10      Min. Z coordinate delimiting object space (cm)   -20.0
11      Max. Z coordinate delimiting object space (cm)    150.0
12      Min. Average Speed (cm/frame)                     0.0
13      Max. Instantaneous Speed (cm/frame)               200.0
14      Max. Size Change of Inelastic Linkages (%)        15.0
15      Min. duration                                     2.0
```

Allowable size change in width or height of a video image   3

True frame rate = 60

```
Target 1 = prox1
Target 2 = dist1
Target 3 = ant1
Target 4 = prox2
Target 5 = dist2
Target 6 = post2
Target 7 = prox3
Target 8 = dist3
Target 9 = post3
```

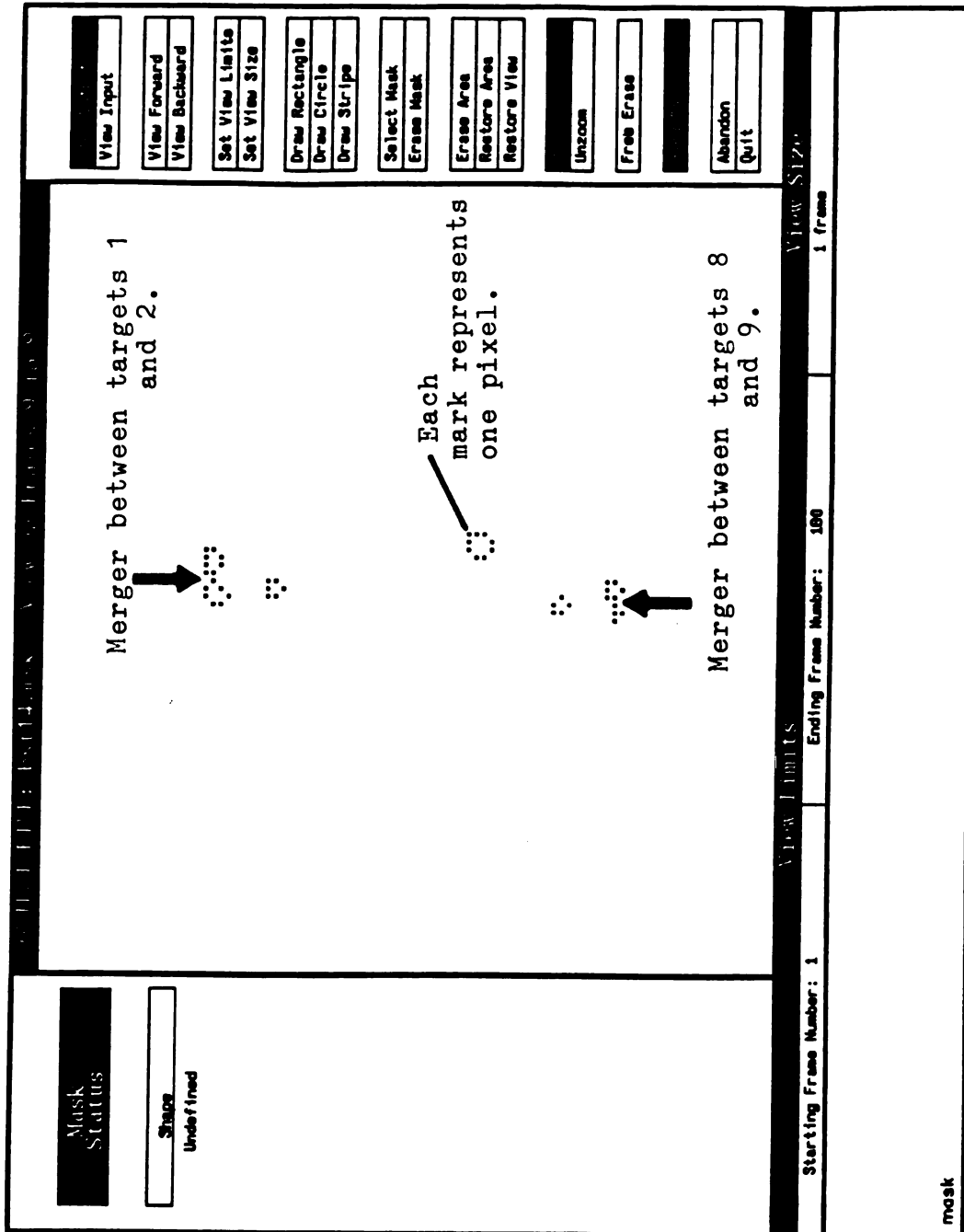Inelastic linkages: 1-2, 2-3, 4-5, 5-6, 7-8, 8-9

30

Figure 4. Sample mergers in the data which were deleted using the "Mask" program within the EV3D program.
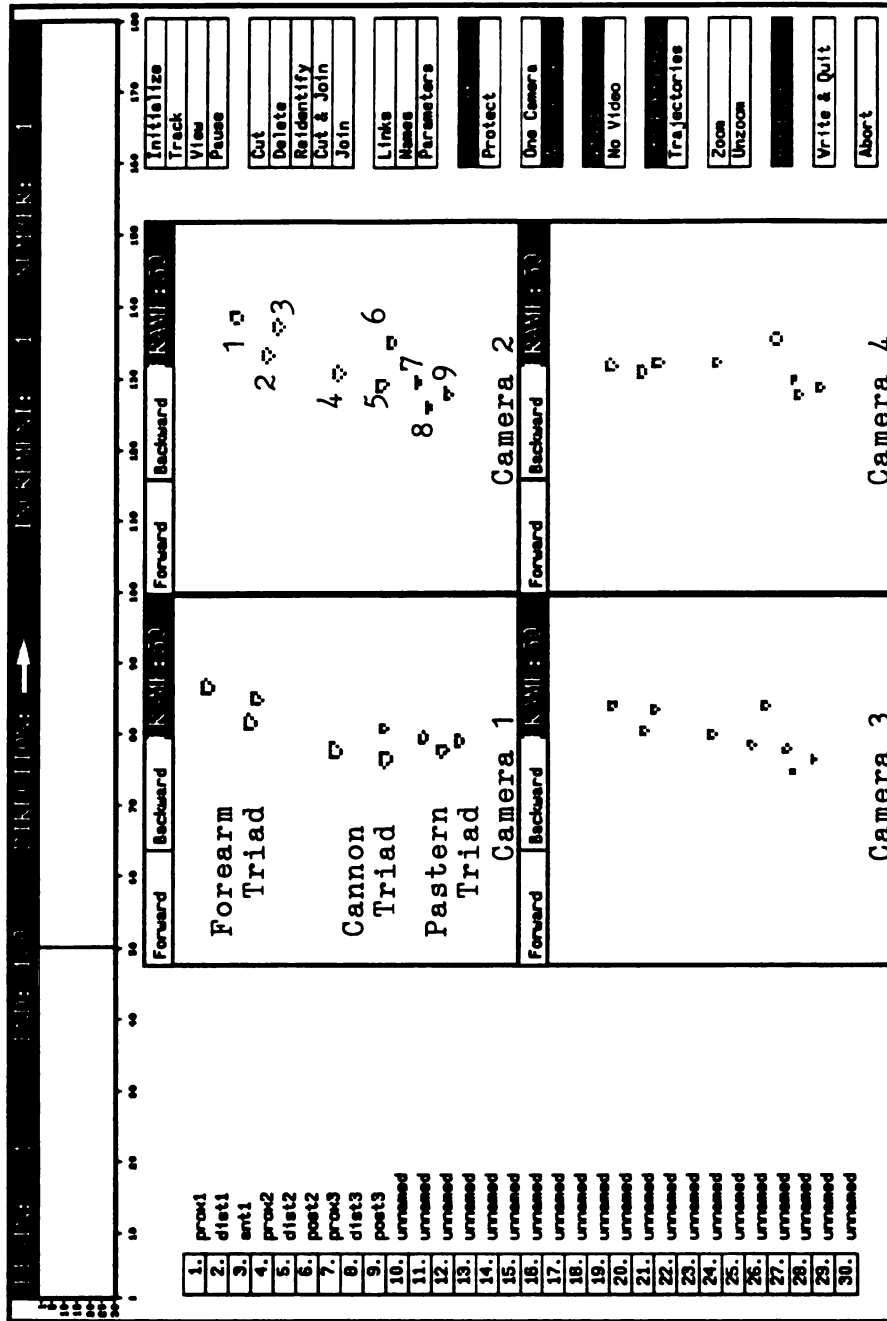
Figure 5. The "Track" program within EV3D showing the 50th frame of data as seen from each camera view.

theoretically, track the data forward or backward through the remaining 179 frames of data. Though these data tracked quite cleanly (compared to other human and canine data tracked with this program), there were still occasional problems. The tracking had to be closely monitored to ensure accuracy. The most commonly encountered problem was with targets seven, eight, and nine. Due to their close proximity, the program would sometimes switch their numbering pattern.

After tracking, the data were "track edited" (see Figure 6). This program showed the trajectory of each of the nine targets in the x, y, and z directions. If there were any gaps in the data or inexplicable deviations, small pieces of data could be removed. However, after masking and carefully tracking, very little track editing was required. Before saving the track edited file, each target path was smoothed through a Tukey Window routine, which is part of EV3D. To double check the track edited file, it was then run through "exam." This program checked to make sure no extraneous data existed and that all target path lengths were equal. A program called "stick" was then run (see Figure 7). This showed the paths of the forearm, cannon, and pastern triads through the gait cycles. Note that while the horse is travelling forward, the leg is travelling through a complete cycle of first backward motion, then forward motion.

Another check was to run the "angle" program. This program calculated the change in angle of a given triad. Since the triads were fixed, the changes were hoped to be
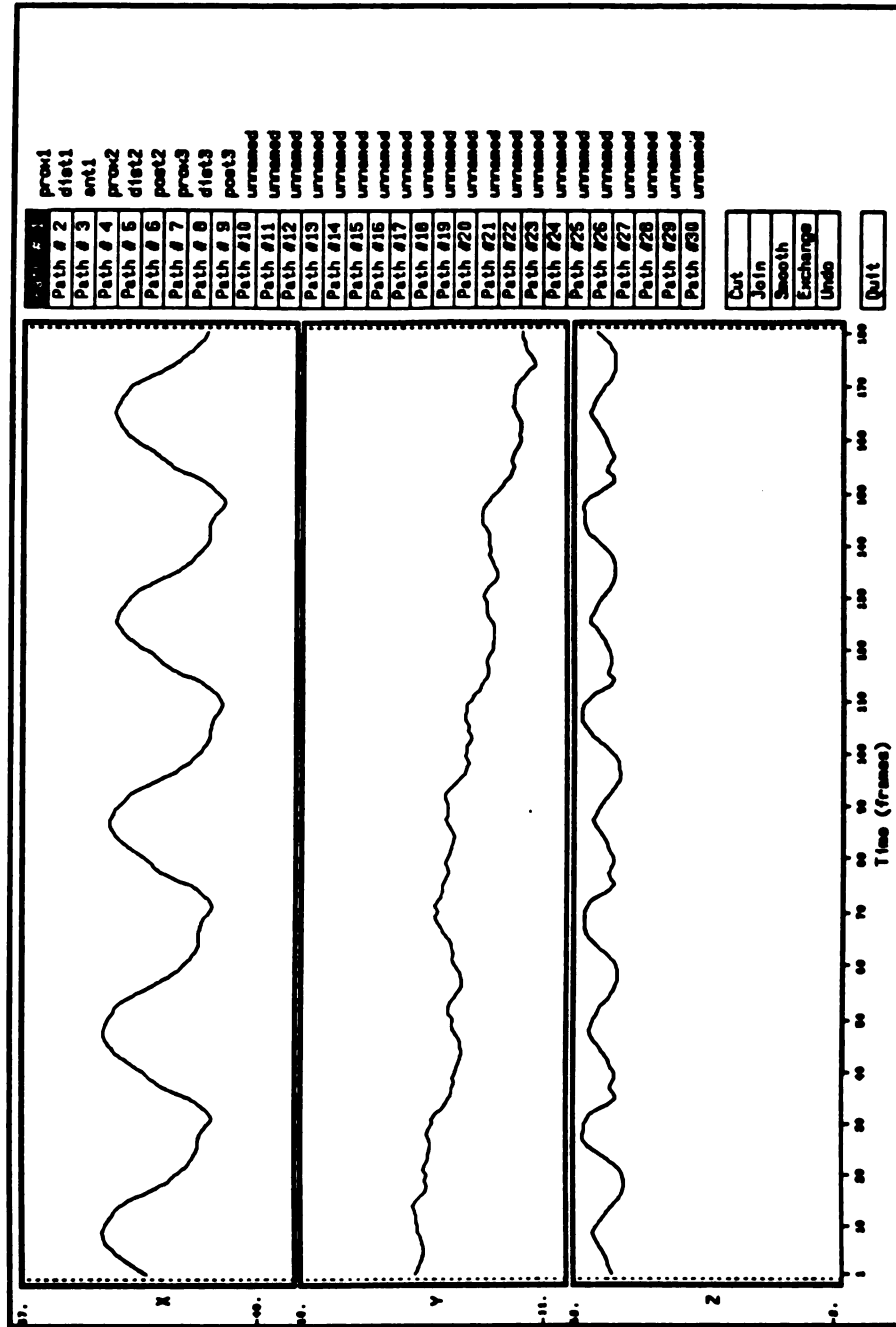
Figure 6. "Track Edit" program within EV3D, demonstrating changes in the x, y, and z trajectories of target 1.
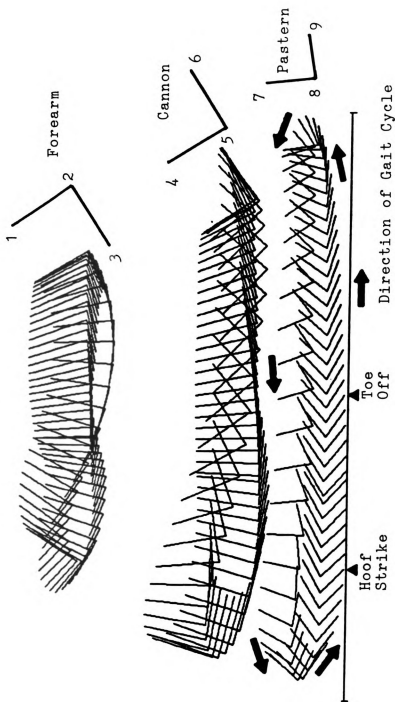
34

Figure 7. Stick diagram of one complete gait cycle. Arrows indicate direction of the gait cycle; the area between hoof strike and toe off represents stance phase; the remainder of the cycle comprises swing phase.

minimal. However, due to the changing of the number of pixels observed in a target as registered in a camera view, it could be expected the calculation would vary a few degrees by calculating different target centroids (see Figure 8). When a tracking mistake was made, though, the difference was sometimes greater than 10°. (Pixels are the tiny square areas which compose any type of television or computer screen.)

Once the files were track edited, they were run through a joint coordinate analysis program. These programs, which were separate from EV3D, were written specifically for the horse's knee and the horse's ankle (MSU Biomechanics Department). These programs were based upon a theory developed by Grood and Suntay (1983) to analyze three-dimensional kinematics of the knee. The theory uses Euler angles (yaw, pitch, and roll as used in engineering theory) to interpret three-dimensional motion of biological systems. Soutas-Little et al. (1987) later used the system to develop a joint coordinate system for the ankle. To our knowledge, this study was the first time a joint coordinate system had been applied to knee and ankle motion of the horse.

The joint coordinates were non-orthogonal (non-perpendicular) systems which allowed non-sequence dependent rotations. Local segment coordinates for the forearm were established in the following manner (see Figures 9 and 10 for coordinate labelling):

$$\hat{z}_f = (\bar{F}_1 - \bar{F}_2)/|\bar{F}_1 - \bar{F}_2|$$

$$\hat{y}_f = [\hat{z}_f \times (\bar{F}_3 - \bar{F}_2)]/|\hat{z}_f \times (\bar{F}_3 - \bar{F}_2)|$$
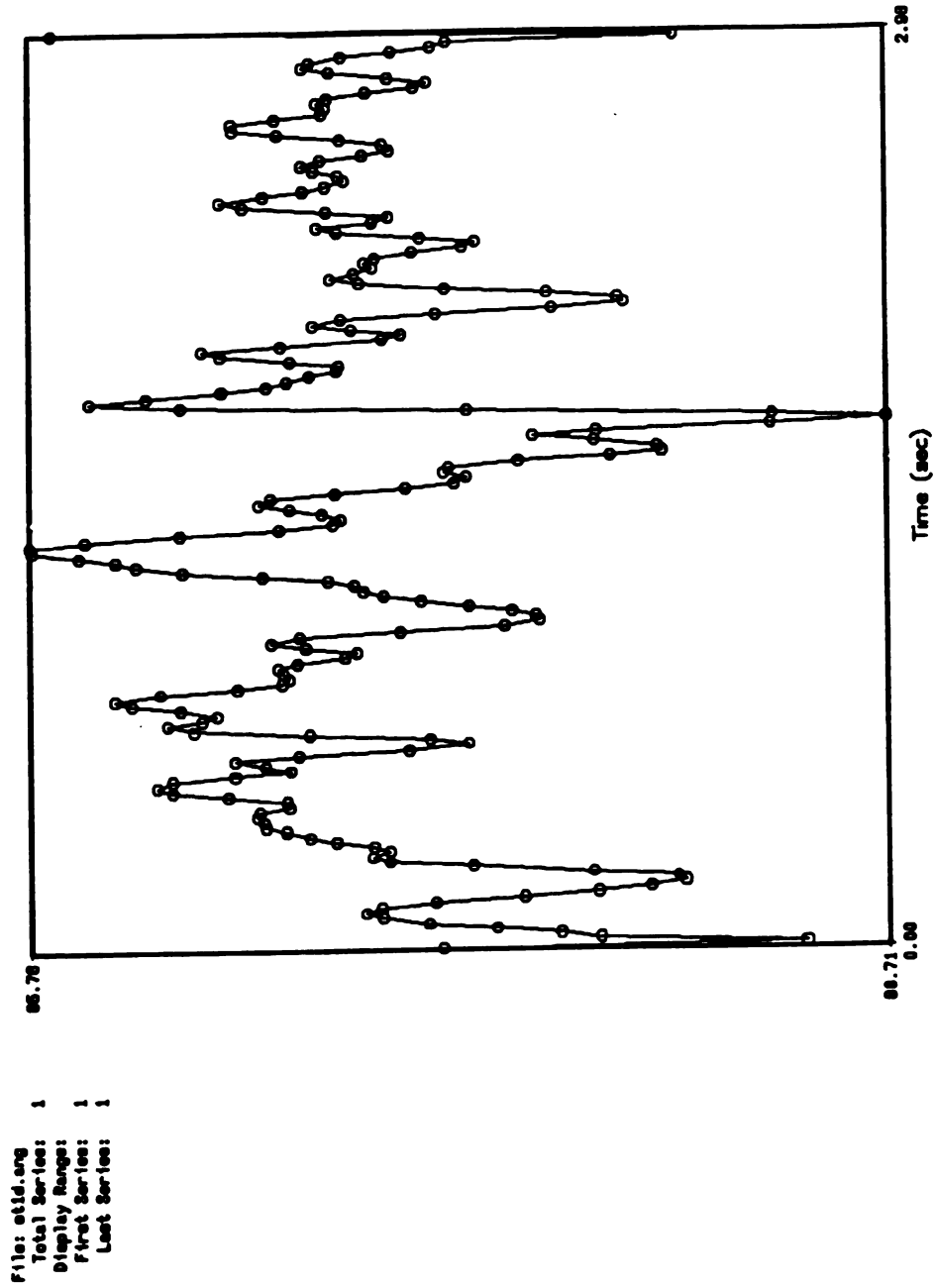
Figure 8. Changes in the angle created by targets 7, 8, and 9. The changes appeared to be based on calculated centroid changes.
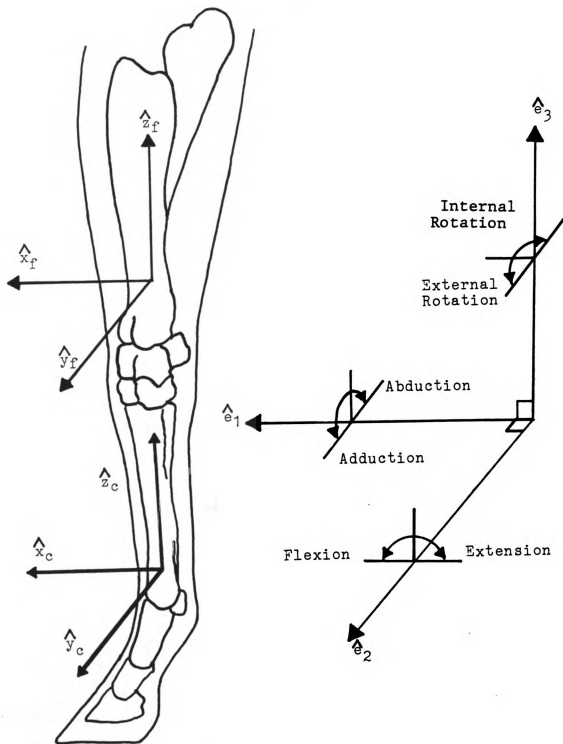
Figure 9. Joint coordinate system for motions of the knee. Motions are of the distal segment relative to the proximal segment (lateral view of left, front leg.)
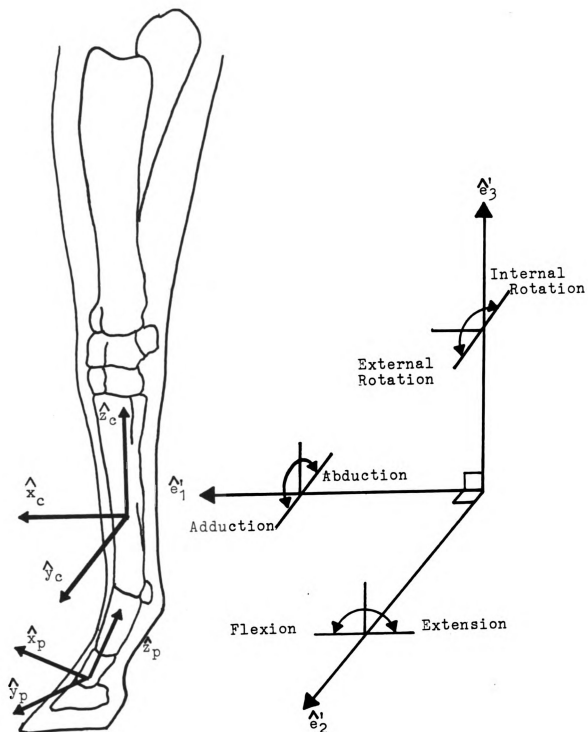
Figure 10. Joint coordinate system for motions of the ankle. Motions are of the distal segment relative to the proximal segment (lateral view of left, front leg.)

$$\hat{x}_f = \hat{y}_f \times \hat{z}_f$$

Local segment coordinates for the cannon:

$$\hat{z}_c = (\bar{C}_4 - \bar{C}_5)/|\bar{C}_4 - \bar{C}_5|$$

$$\hat{y}_c = [\hat{z}_c \times (\bar{F}_5 - \bar{F}_6)]/|\hat{z}_c \times (\bar{F}_5 - \bar{F}_6)|$$

$$\hat{x}_c = \hat{y}_c \times \hat{z}_c$$

Local segment coordinates for the pastern:

$$\hat{z}_p = (\bar{P}_7 - \bar{P}_8)/|\bar{P}_7 - \bar{P}_8|$$

$$\hat{y}_p = [\hat{z}_p \times (\bar{P}_8 - \bar{P}_9)]/|\hat{z}_p \times (\bar{P}_8 - \bar{P}_9)|$$

$$\hat{x}_p = \hat{y}_p \times \hat{z}_p$$

Joint angles for the knee joint were designed with the flexion/extension axis being $\hat{y}_f$ and internal/external rotation being defined about $\hat{z}_c$. The joint coordinates were:

$$\hat{e}_2 = \hat{y}_f \quad \text{Flexion and extension}$$

$$\hat{e}_3 = \hat{z}_c \quad \text{Internal and external rotation}$$

$$\hat{e}_1 = (\hat{e}_2 \times \hat{e}_3)/|\hat{e}_2 \times \hat{e}_3| \quad \text{Abduction and adduction}$$

The joint Euler angles were:

Flexion/extension $= -\sin^{-1}(\hat{e}_1 \cdot \hat{z}_f)$ Flexion is positive.

Abduction/adduction $= \sin^{-1}(\hat{e}_2 \cdot \hat{e}_3)$ Abduction is positive.

Internal/external rotation $= \sin^{-1}(\hat{e}_1 \cdot \hat{y}_c)$ Internal rotation is positive. These angles were of the cannon relative to the forearm, or the distal segment relative to the proximal segment.

Joint angles for the ankle joint were designed with the flexion/extension axis being $\hat{y}_c$ and internal/external rotation being defined about $\hat{z}_p$. Pastern coordinates were rotated in the program so as to be perpendicular to the cannon

coordinates. The joint coordinates were:

$\hat{e}_2{}' = \hat{y}_c$ Flexion and extension

$\hat{e}_3{}' = \hat{z}_p$ Internal and external rotation

$\hat{e}_1{}' = (\hat{e}_2{}' \times \hat{e}_3{}')/|\hat{e}_2{}' \times \hat{e}_3{}'|$ Abduction and adduction

The joint Euler angles were:

Flexion/extension $= -\sin^{-1} (\hat{e}_1{}' \cdot \hat{z}_c)$ Flexion is positive.

Abduction/adduction $= -\sin^{-1} (\hat{e}_2{}' \cdot \hat{e}_3{}')$ Abduction is positive.

Internal/external rotation $= \sin^{-1} (\hat{e}_1{}' \cdot \hat{y}_p)$ Internal rotation is positive.

These equations were written into a computer program to facilitate faster analysis of the otherwise cumbersome matrix algebra (see Appendix 1 for an example of the hand calculations for one frame of data). After the data were run through the joint coordinate analyses programs, they were plotted to allow visual examination of flexion/extension, abduction/adduction, and internal/external rotation.

RESULTS AND DISCUSSION

Since the joint coordinate analysis (JCA) computer programs were newly written for the horse, a method was needed to check the accuracy of the curves generated. The EV3D program allowed for angle calculation between rigid bodies. Flexion/extension graphs were thus generated by this method (Figures 11 and 12). Figure 11 shows flexion/extension between the forearm and the cannon, which corresponds to
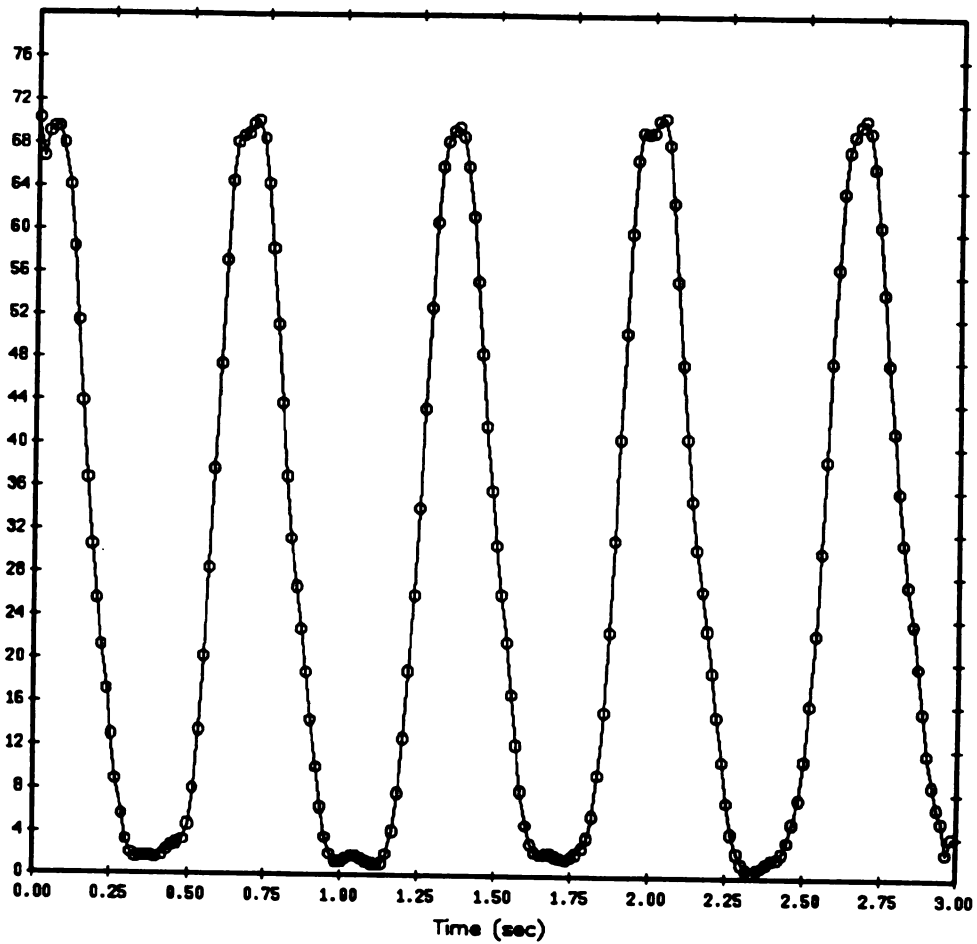
Figure 11. EV3D generated flexion/extension curve of subject BS's knee while trotting. Peak areas represent maximum flexion, Low areas represent stance phase.
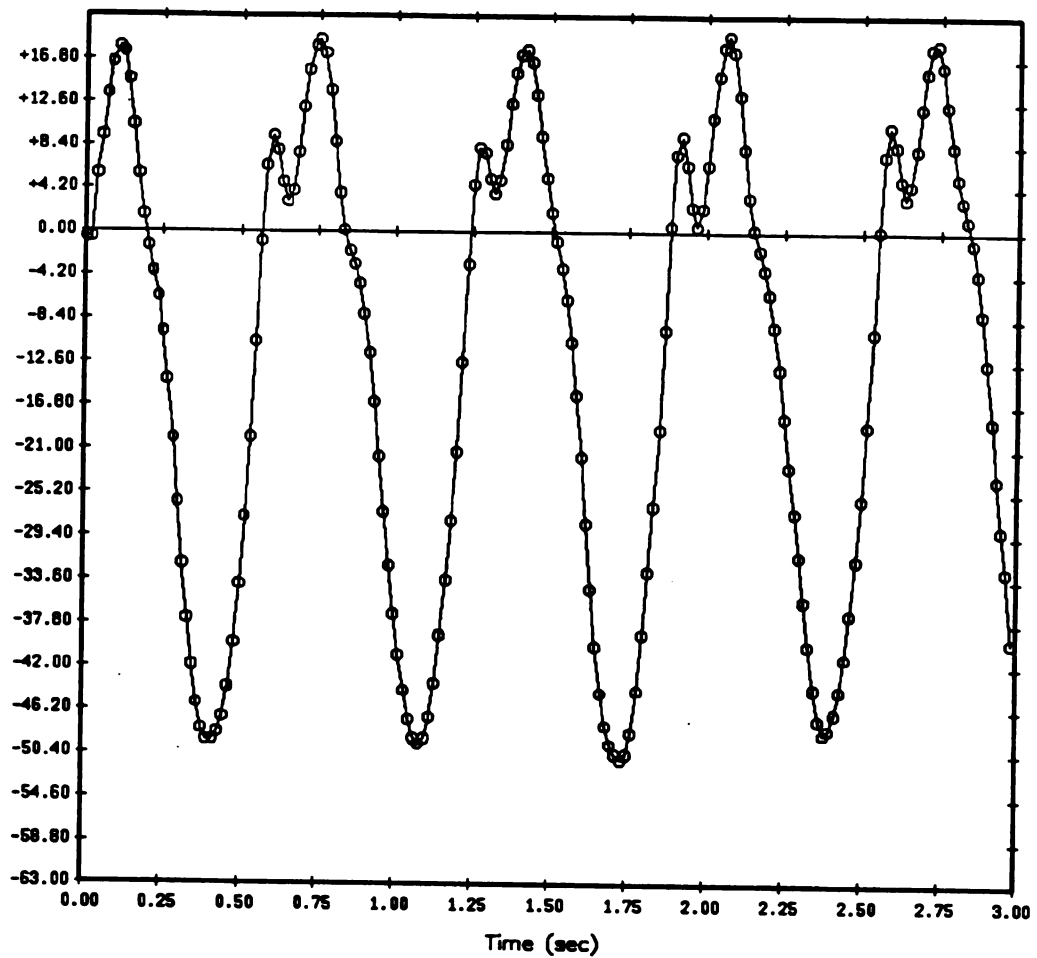
Figure 12. EV3D generated flexion/extension curve of
subject BS's ankle while trotting. Peak areas represent
maximum flexion. Low areas represent stance phase.

flexion/extension of the knee. Figure 12 shows flexion/extension between the cannon and the pastern, which corresponds to flexion/extension of the ankle. When these graphs were compared to the flexion/extension curves generated by the JCA programs (e.g. Figures 18 and 19), the results were nearly identical, both in ranges of motion and shapes of curves. Since the calculated JCA flexion/extension curves matched the EV3D generated curves for flexion/extension, this was a good indication that the calculated abduction/adduction and internal/external rotation would also be correct.

Because the MSU Veterinary Clinical Center facilities do not have a force plate at this time, identifying hoof strike (when the hoof first comes in contact with the ground) and toe off (when the hoof first loses contact with the ground) was less precise than would have been ideal. Consequently, stance phase (when the hoof is in contact with the ground) was more estimated than exact. Stick figures of the gait cycles were generated and compared to standing position data. These, along with watching the stick figures during gait cycles, helped clarify where hoof strike and toe off occurred (Figure 13).

Upon examining the flexion/extension curves (Figures 11, 12, 16, 17, 18, 20, 23, 24, 25, and 26), stance phase can be described as the low areas between the peaks. Since more hyperextension occurred in the ankle than in the knee (as could be observed visually), this coincided with the finding that extension went lower after hoof strike in the ankle than
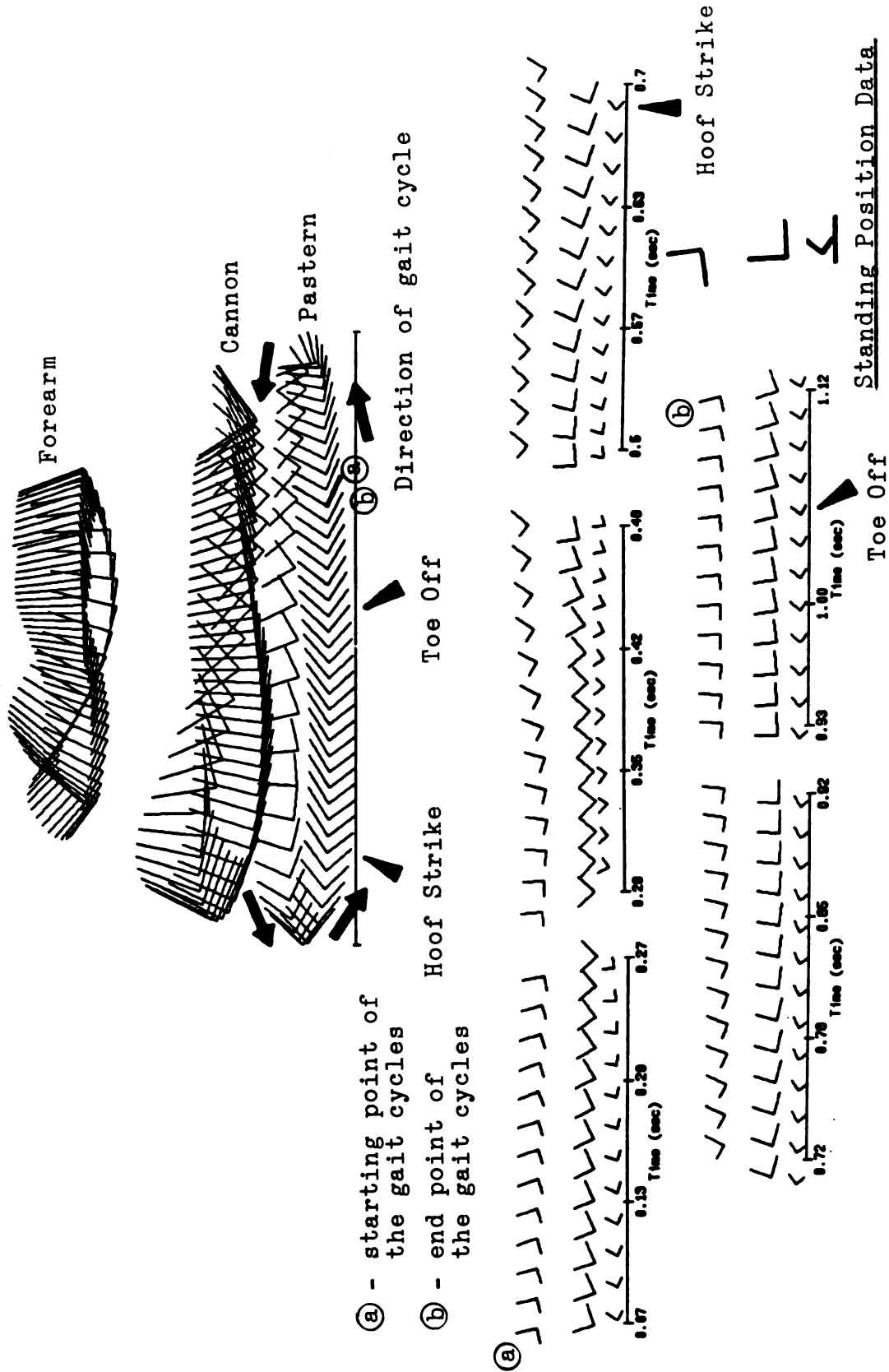
Figure 13. A sample walking trial examined with stick figures in one gait cyle, and then broken down by time. These types of figures helped identify hoof strike and toe off.

in the knee.

When evaluating the standing data (Figures 14, 15, 21, and 22), it should be noted that subtle deviations in the kinematic patterns occur due to the subjects shifting weight from side to side and fidgeting. Also, in the graph legends, several abbreviations are used: Abd+ means abduction occurs in the positive direction, or upwards; Add- means adduction occurs in the negative direction, or downwards; Flex+ means flexion occurs in the positive direction; Ext- means extension occurs in the negative direction; IntR+ means internal rotation occurs in the positive direction; ExtR- means external rotation occurs in the negative direction.

Upon examining the graphs of movement (Figures 16, 17, 18, 20, and 23-26), it is noteworthy that stride repeatability was very high, not only within each trial, but from trial to trial. This can be checked by examining the curve shapes for each gait cycle and comparing the peaks of the gait cycles. This was particularly noticeable with the flexion/extension graphs. Internal and external rotation appeared to be the least repeatable graphs, although definite patterns existed. This apparent lowered repeatability could be artificial, however, due to the fact that there is a comparatively small range of motion ($^\sim 10^{\circ}$) taking place in this plane. The overall repeatability that was observed helped document that the methodology chosen for this study was effective for analyzing flexion/extension, abduction/adduction, and internal/external rotation of the knee and ankle joints. Had
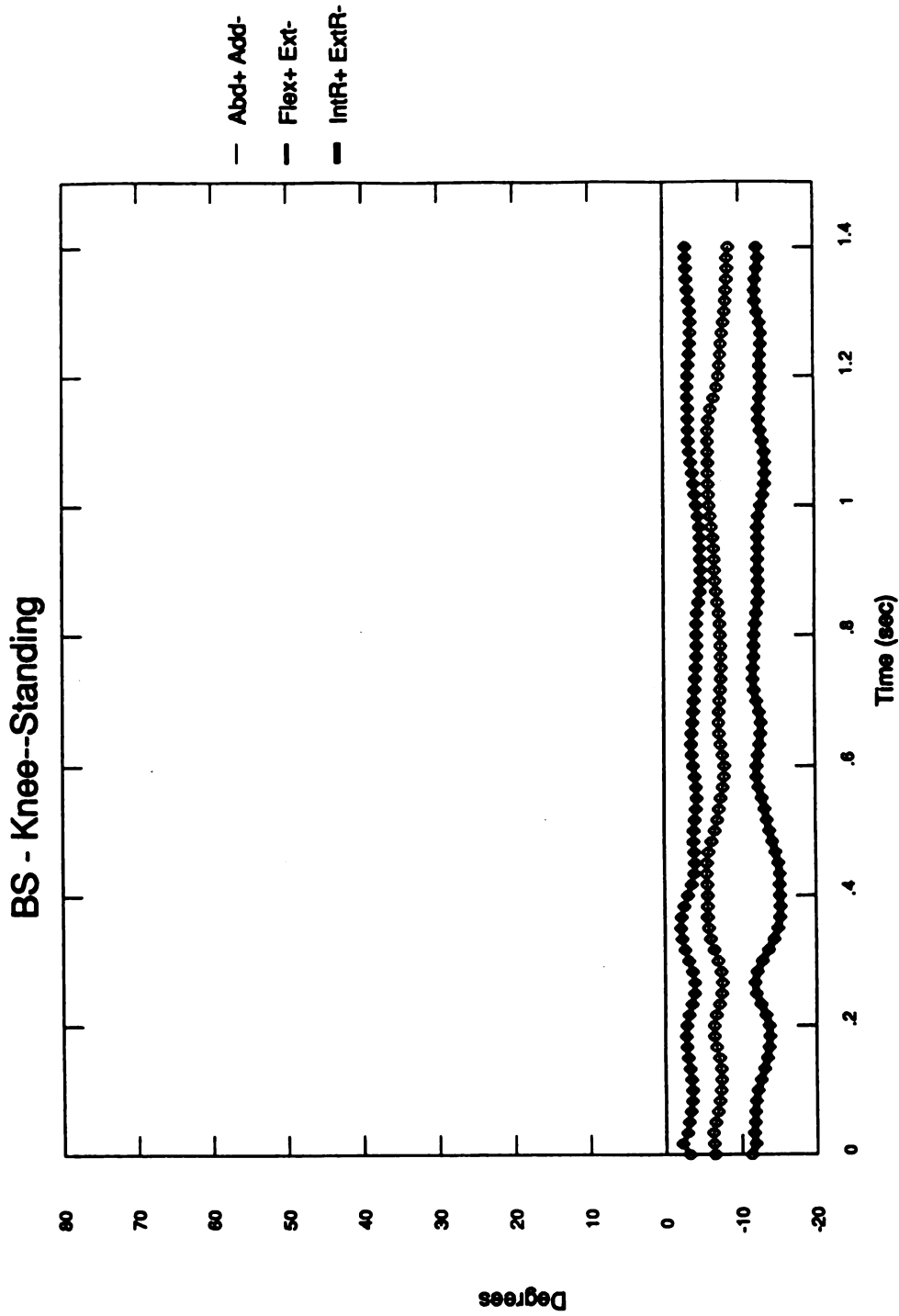
Figure 14. Kinematics for the knee joint. "Abd+" means abduction occurs in the positive direction; "Add-" means adduction occurs in the negative direction. "Flex+" means flexion occurs in the positive direction; "Ext-" means extension occurs in the negative direction. "IntR+" means internal rotation occurs in the positive direction; "ExtR-" means external rotation occurs in the negative direction.
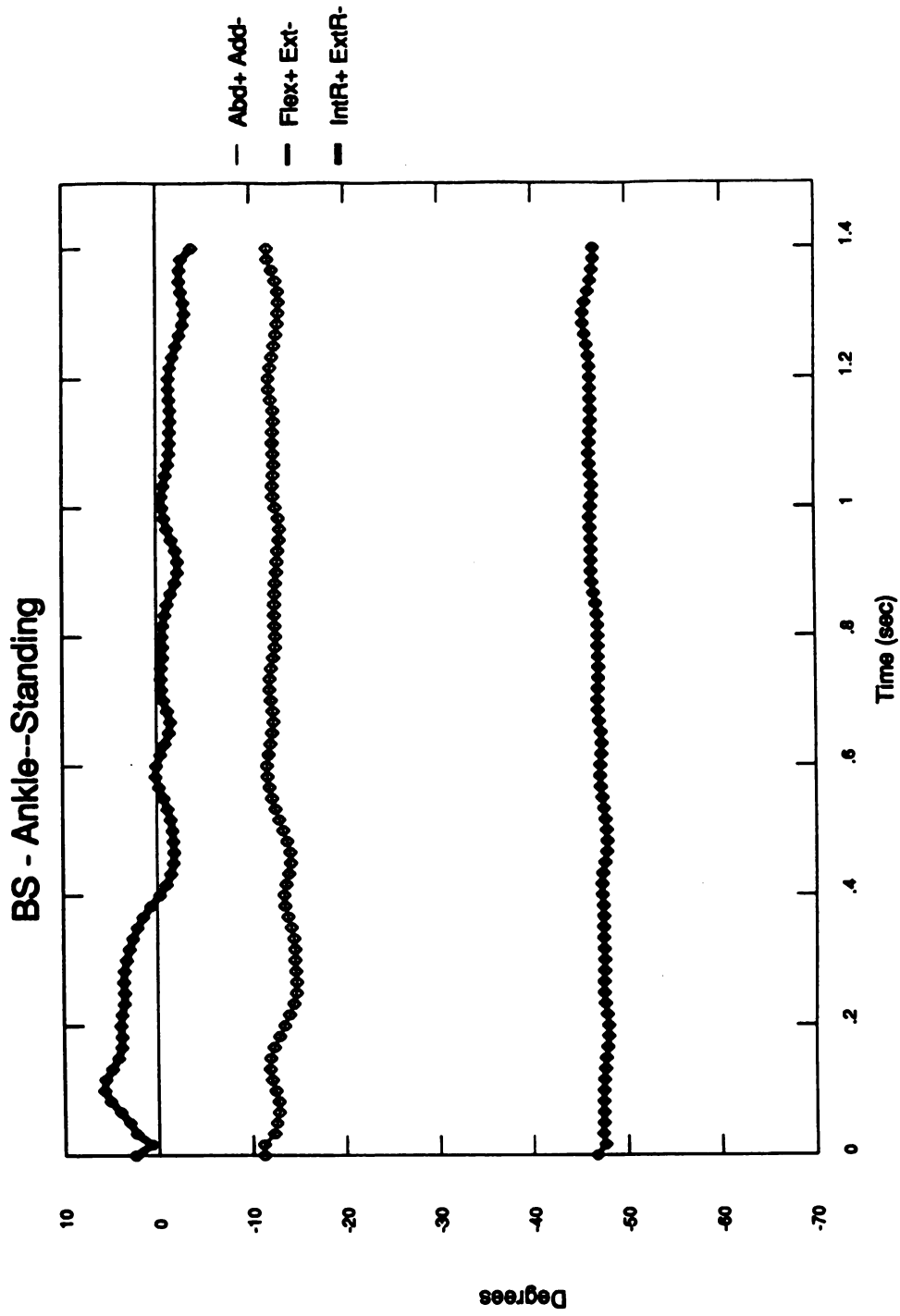
Figure 15. Kinematics for the ankle joint. Slight deviations in the standing data are due to the subject shifting weight.
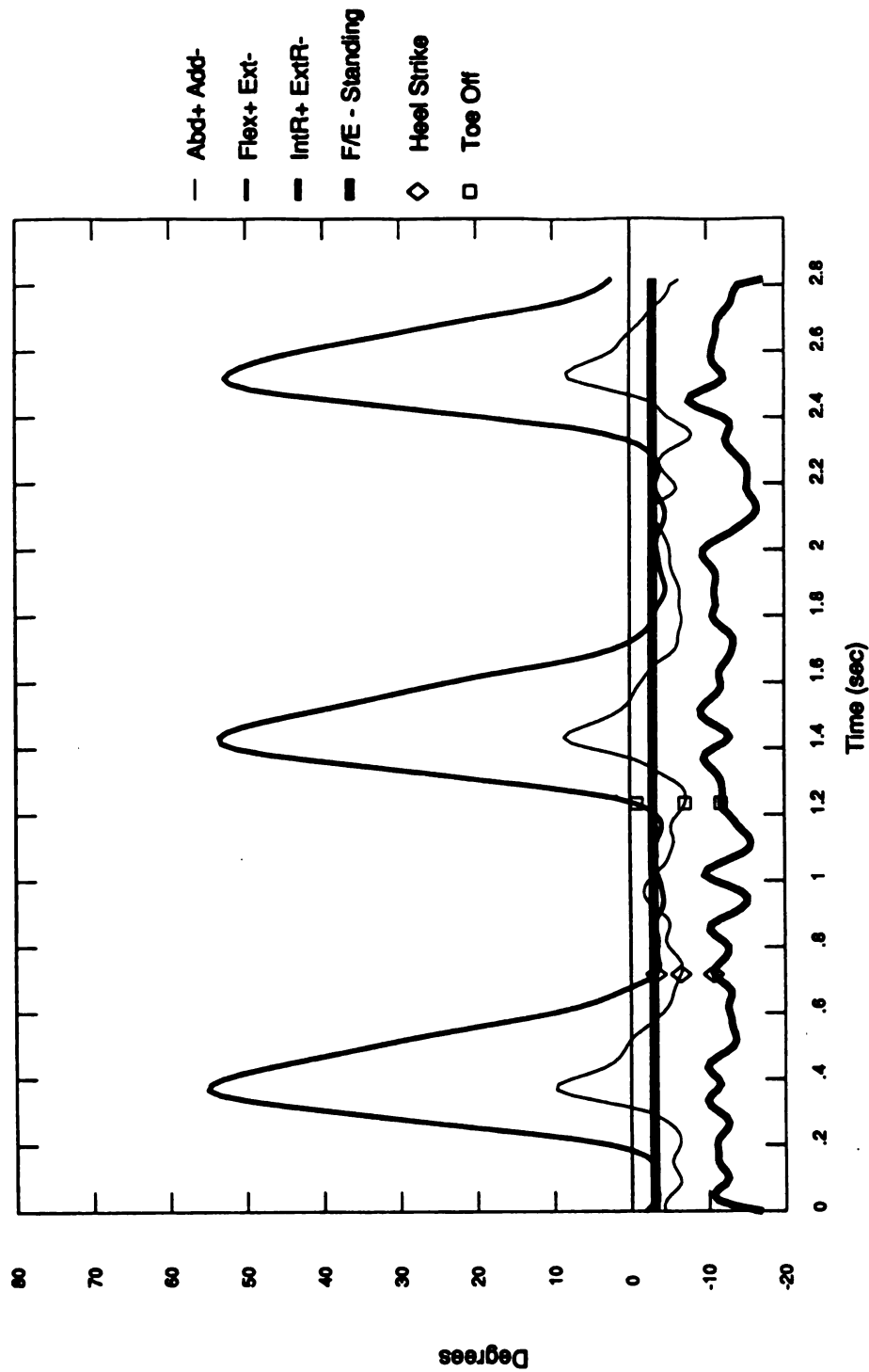
Figure 16. Kinematics for the knee joint. The legend is the same as that in Figure 14 with the addition of hoof strike (labelled heel strike) and toe off being marked in the first gait cycle. "F/E-Standing" gives the average standing value for flexion/extension.
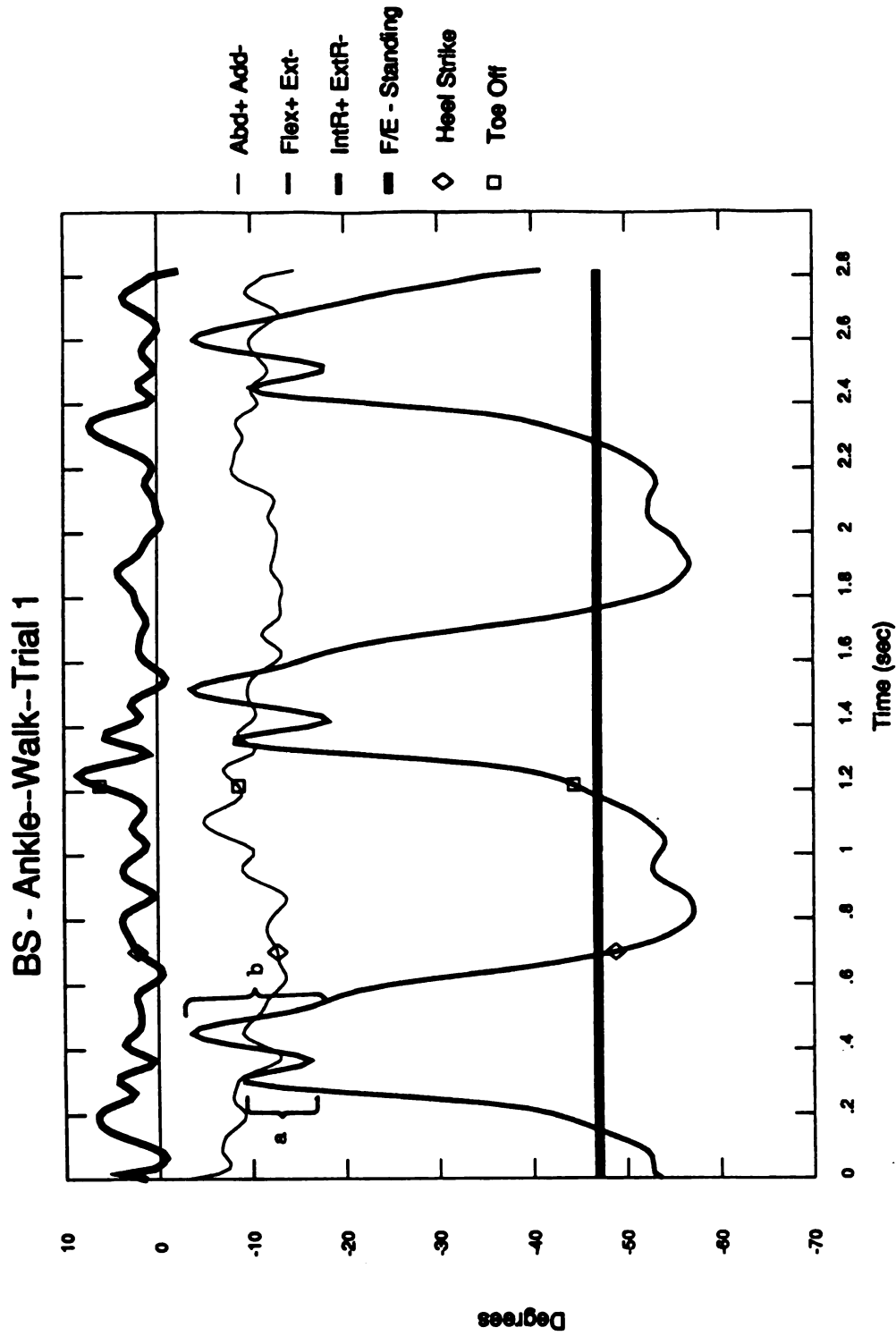
Figure 17. Kinematics for the ankle joint. The legend is further described in Figures 14 and 16. The first peak of flexion is referred to as "a." The second peak of flexion is referred to as "b."

there been a tremendous variation between gait cycles, it might have indicated that there was too much wobble in the targeting scheme or that the calibration area had been improperly selected. In addition, the treadmill proved to be a good tool for gait analysis since more than one gait cycle could be viewed in each trial. Typically, four gait cycles were filmed in each trotting trial, and three gait cycles were filmed in each walking trial. These multiple trials also helped in evaluating stride repeatability.

Graphs were very similar from trial to trial; therefore, a representative graph was chosen for each condition for each subject; i.e., one standing, knee; one standing, ankle; one walking, knee; one walking, ankle; one trotting, knee; and one trotting, ankle (Figures 14-18 and 20-26). Not all curves extend the entire three seconds that filming was conducted. Data tended to be less predictable toward the beginning and the end of the trials, so the ends of some trials were clipped. (This phenomenon of lowered accuracy at either end of the file has been observed in many human and canine trials as well.) Standing files were edited to 1.5 seconds since there were no gait cycles to be concerned with.

To begin with, Figure 18 will be analyzed in a step by step manner. To review, flexion occurs when the angle between two body segments becomes smaller, and extension occurs when the angle between two body segments becomes larger. Abduction occurs when a body segment, in this study the distal segment relative to the proximal segment, is moved away from the
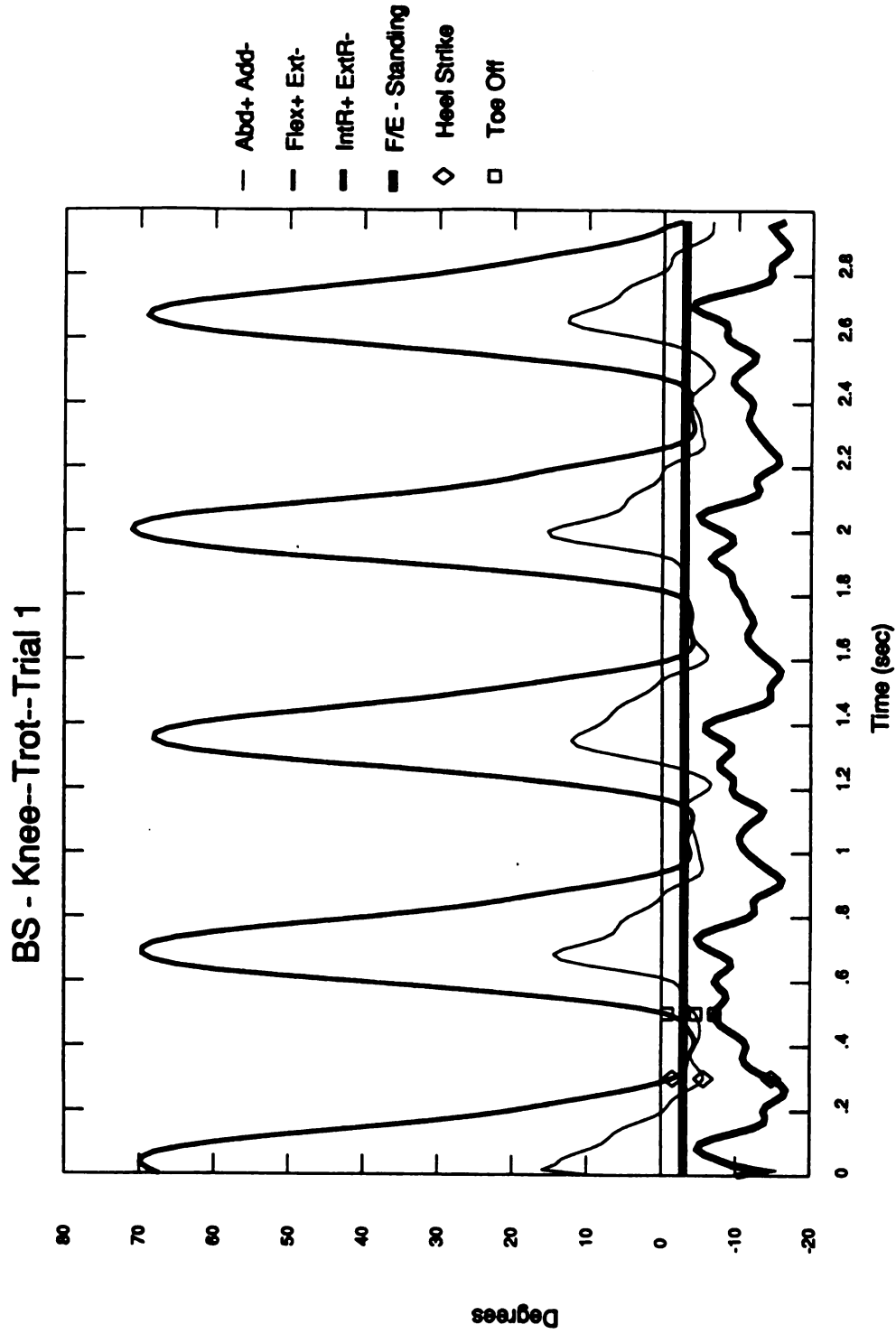
Figure 18. Kinematics of the knee joint. The legend is further described in Figures 14 and 16. Each trial represented was chosen as being exemplary of the three trials filmed for each particular condition.
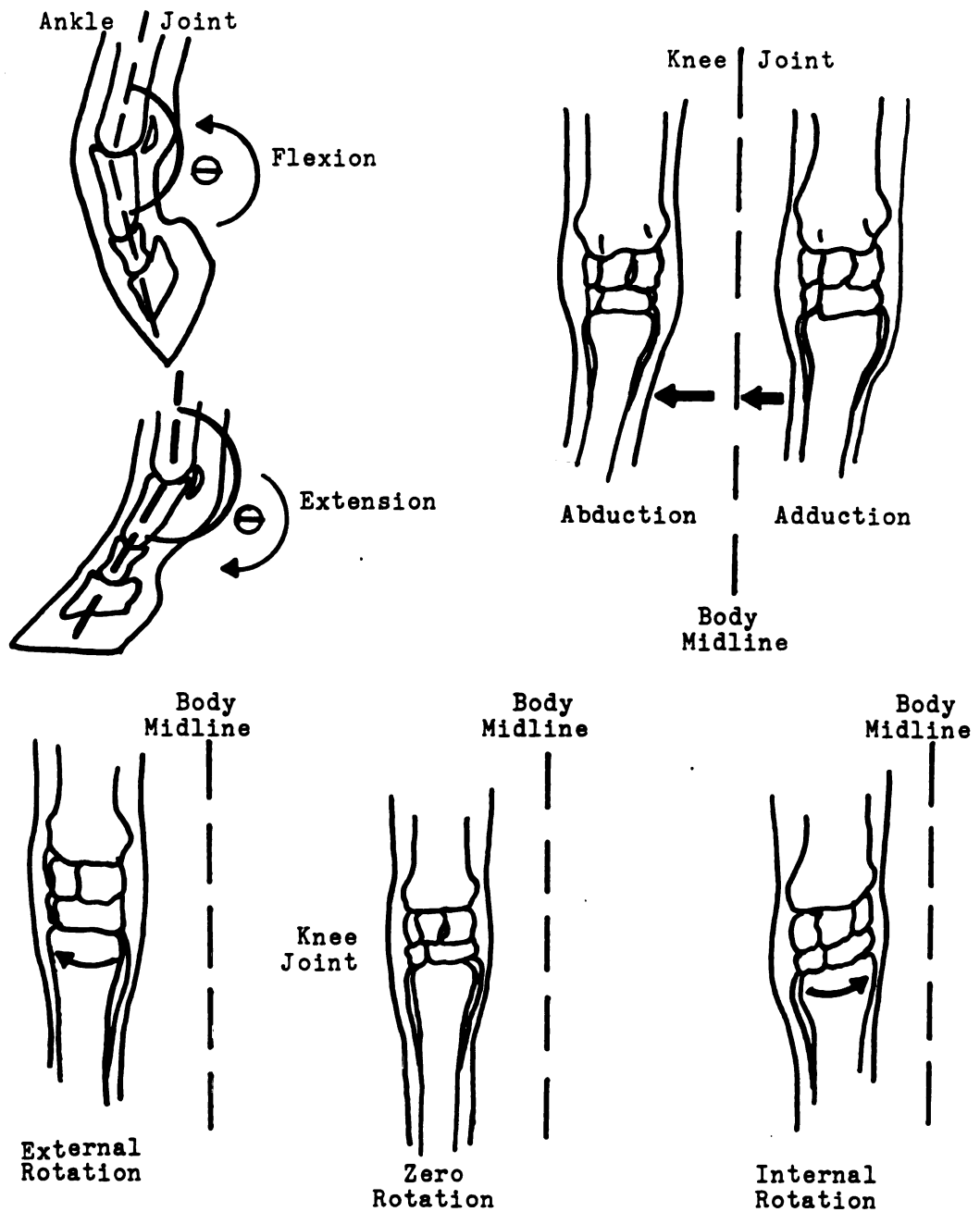
Figure 19. Descriptive drawings of the motions being described.
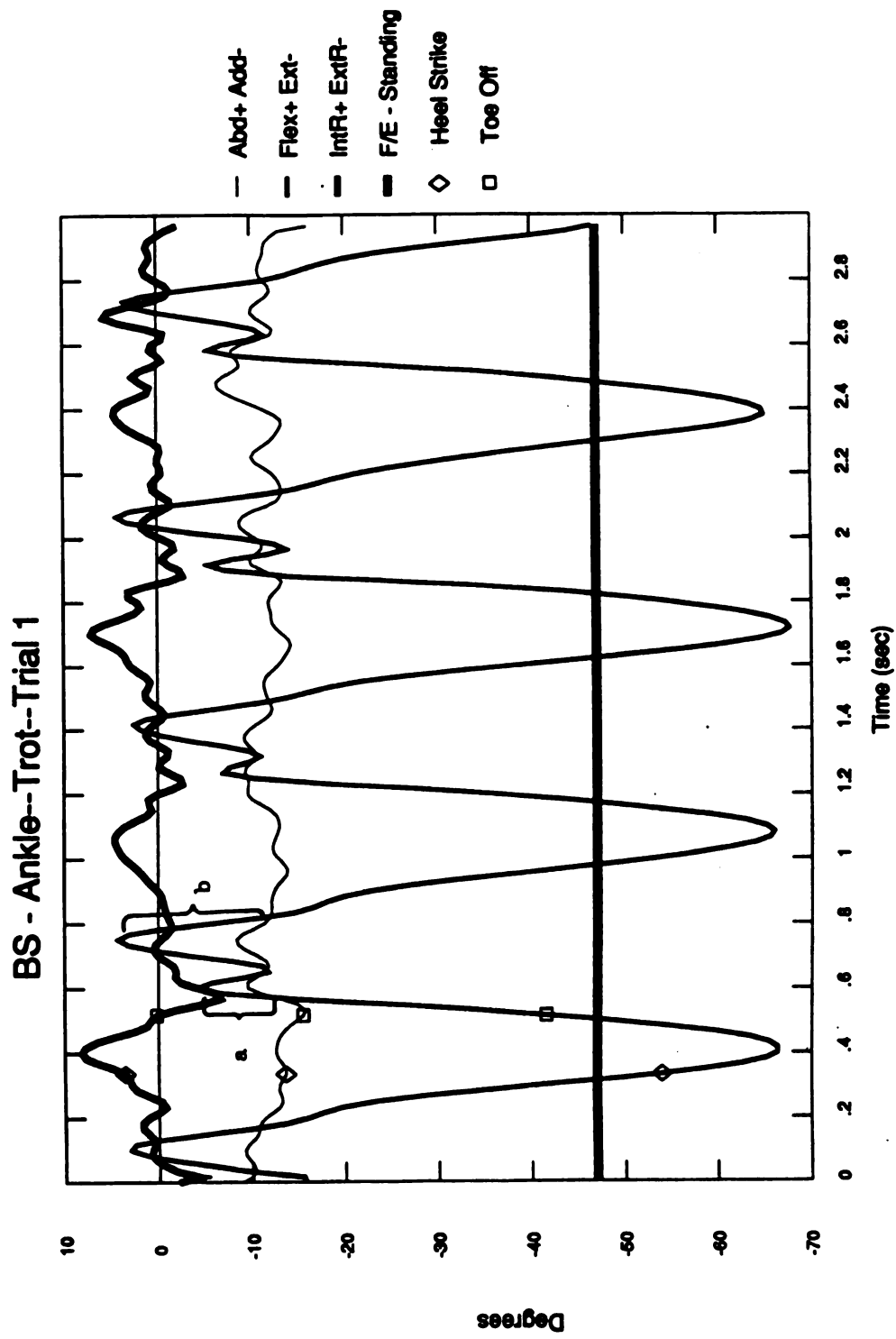
Figure 20. Kinematics of the ankle joint. The legend is further described in Figures 14 and 17.

body's midline. Adduction occurs when the segment moves toward the body's midline. Internal rotation takes place when a joint rotates inwardly, i.e., toward the body midline, or, for example, the left knee rotates towards the right. External rotation occurs when a joint rotates outwardly, i.e., away from the body midline, or, for example, the left knee rotates toward the left (Figure 19).

The curve showing the greatest range of motion, represented by the medium width line, depicts flexion and extension. In this particular figure, the knee of subject BS is represented. Action occurring upward, i.e., in the positive direction, indicates that the knee was flexing. Action going downward, i.e., in the negative direction, means the knee was extending. Note that while a zero point is represented, there has been no standard definition of where "zero" is for gait analysis. If these data were compared to data performed under different methodology, it would be more important to compare the shapes of the curves and the ranges of motion than the zero points. Average standing data values for flexion/extension have been identified on the appropriate graphs to also use as a basis of comparison.

Hoof strike and toe off have been marked on the first gait cycle of each graph. Since the graphs were generated using human plotting programs, hoof strike on the figures in referred to in the legend as "heel strike." The areas between hoof strike and toe off represent approximate stance phase for all gait cycles. From toe off until the next hoof strike

represents swing phase. (Stance phase is when the hoof is in contact with the ground; swing phase is when the leg is in flight.)

Continuing with the analysis of Figure 18, as the subject flexed the knee, the lower leg was abducted, which is represented by the fine line. At maximum flexion, the knee was as internally rotated as it would be. As the knee extended back toward stance phase, the lower leg was adducted, as well as being externally rotated.

The ankle graph of this same trial, Figure 20, depicts highly superimposable curves, i.e. both knee and ankle were reaching flexions and extensions at nearly identical times. The first peak of flexion will be referred to as peak "a." The second peak of flexion will be referred to as peak "b." This double peak flexion is an interesting phenomenon that was at first thought to be a mistake. After all ankle graphs were plotted and had demonstrated some form of double peak flexion, the stick figures were reanalyzed. The modest extension between the peaks seems to occur as the cannon moved forward over the ankle joint before the ankle would start to flex again.

In comparing the walk to the trot, beginning with subject BS's knee (Figures 16 and 18), the curve shapes are quite similar. The primary differences were in range of motion and length of time for completion of each gait cycle. The range of motion for flexion/extension at the walk was approximately 60°. Range of motion for flexion/extension at the trot was

approximately 75°. Ranges of motion for abduction/adduction and internal/external rotation were also greater at the trot that at the walk. The number of frames, or time, taking for swing phase was more similar between the walk and trot than was the time taking for stance phase. Stance phase at the trot took approximately 0.20 seconds to complete. Stance phase at the walk took approximately 0.55 seconds. Swing phase took approximately 0.45 seconds at the trot and approximately 0.50 seconds at the walk.

In comparing the walk to the trot with subject EC's knee (Figures 23 and 25), the curve shapes were again quite similar. The range of motion for flexion/extension at the walk was approximately 63°. The range of motion for flexion/extension at the trot was approximately 76°. Ranges of motion for abduction/adduction and internal/external rotation did not differ as much between the walk and trot as they did for subject BS. Timing lengths for stance phase and swing phase were quite similar to those of subject BS, again differing primarily in stance phase length.

Regarding subject BS's ankle graphs (Figures 17 and 20), there were more differences in shape than had been observed in the knee. The first flexion peak will be referred to as peak "a," and the second flexion peak will be referred to as peak "b." At the walk, peak "a" was a larger percentage of "b" than what occurred at the trot. Also at the walk, during stance phase, there was a subtle flexion at approximately midstance. This appears not to have happened at the trot.

Figure 21. Kinematics for the knee joint. See Figure 14 for further explanation of the legend.

Figure 22. Kinematics for the ankle joint. See Figure 14 for further explanation of the legend.

Figure 23. Kinematics for the knee joint. The legend is further described in Figures 14 and 16.

Figure 24. Kinematics for the ankle joint. See Figure 14 and 17 for further explanation of the legend.
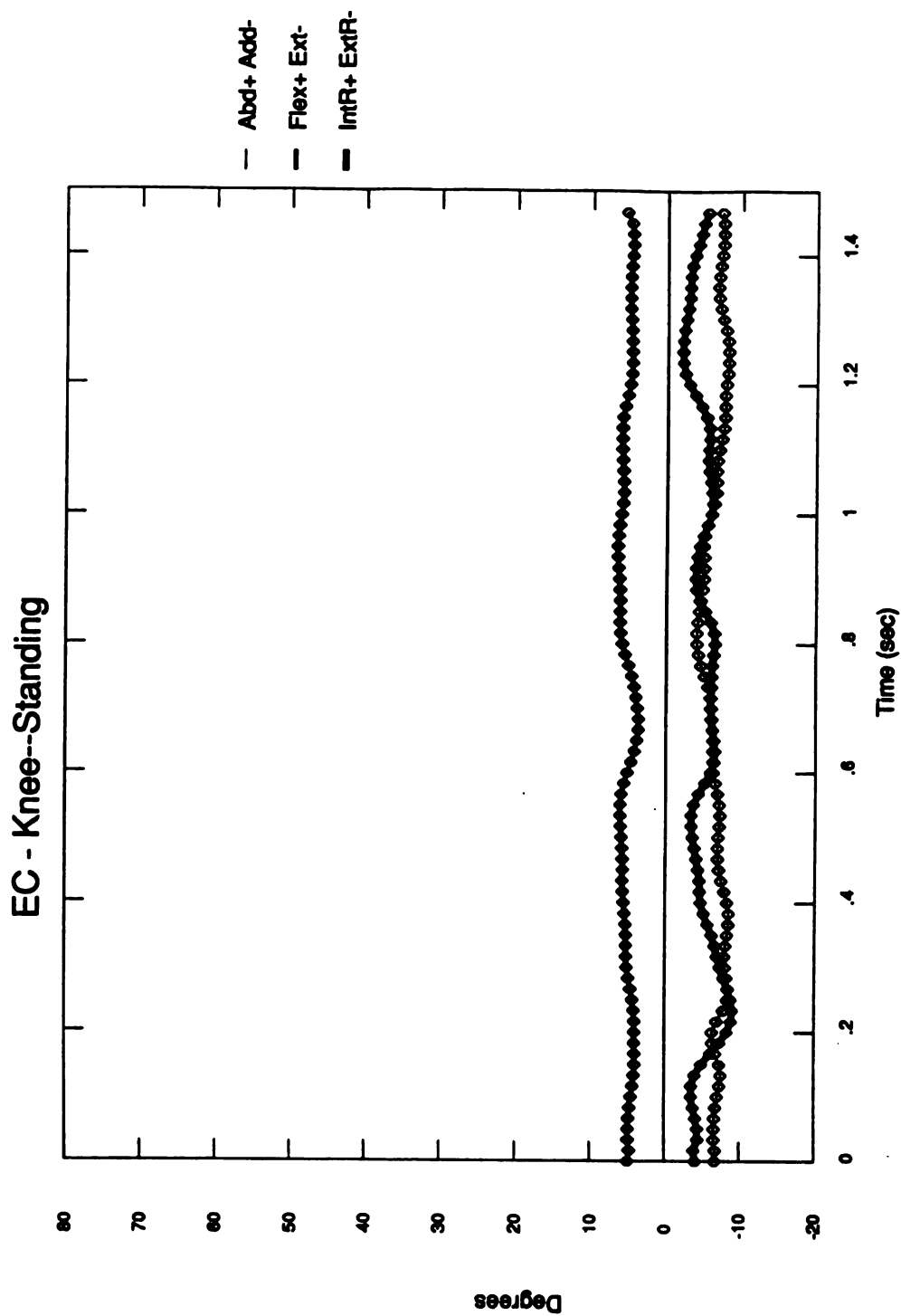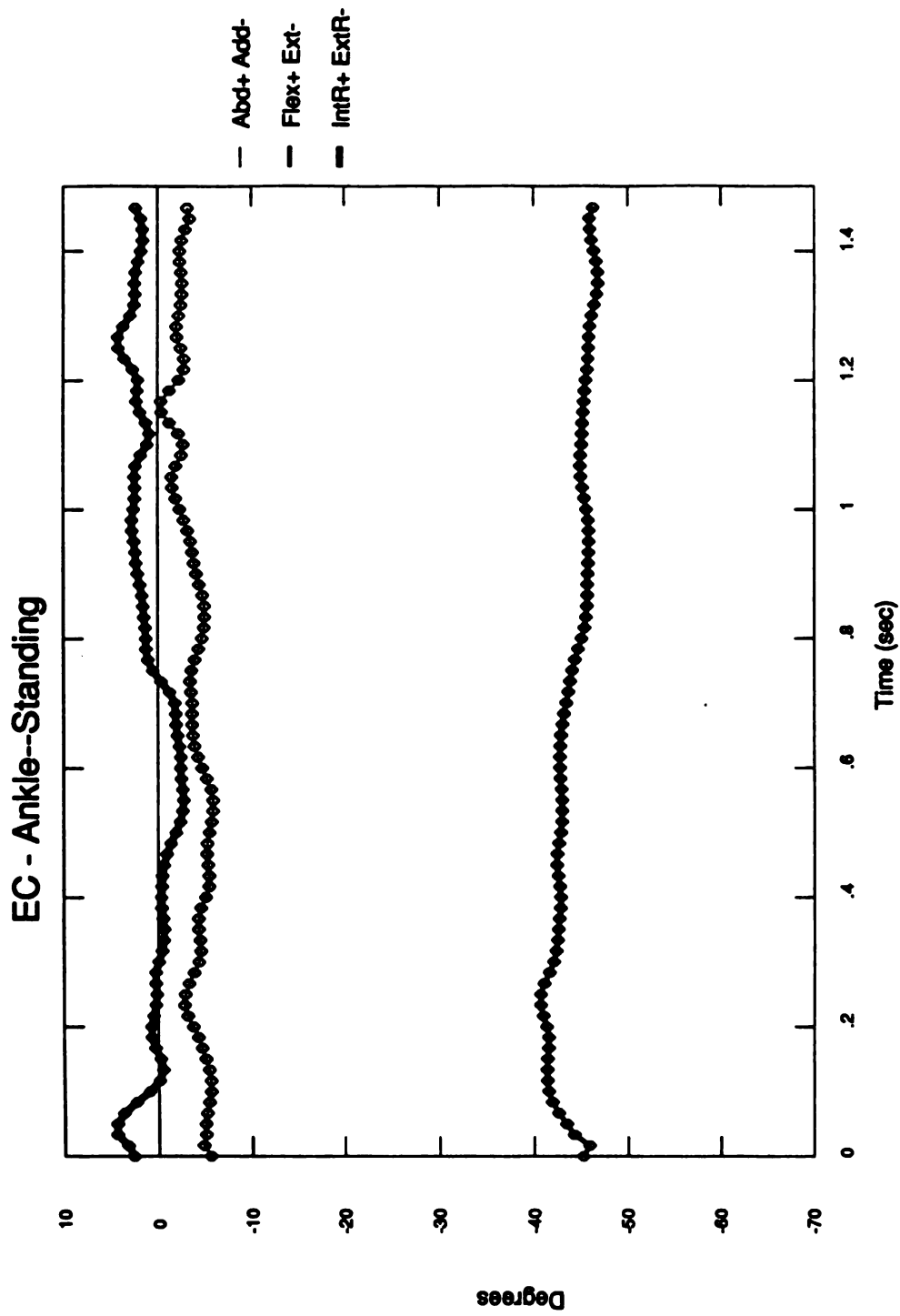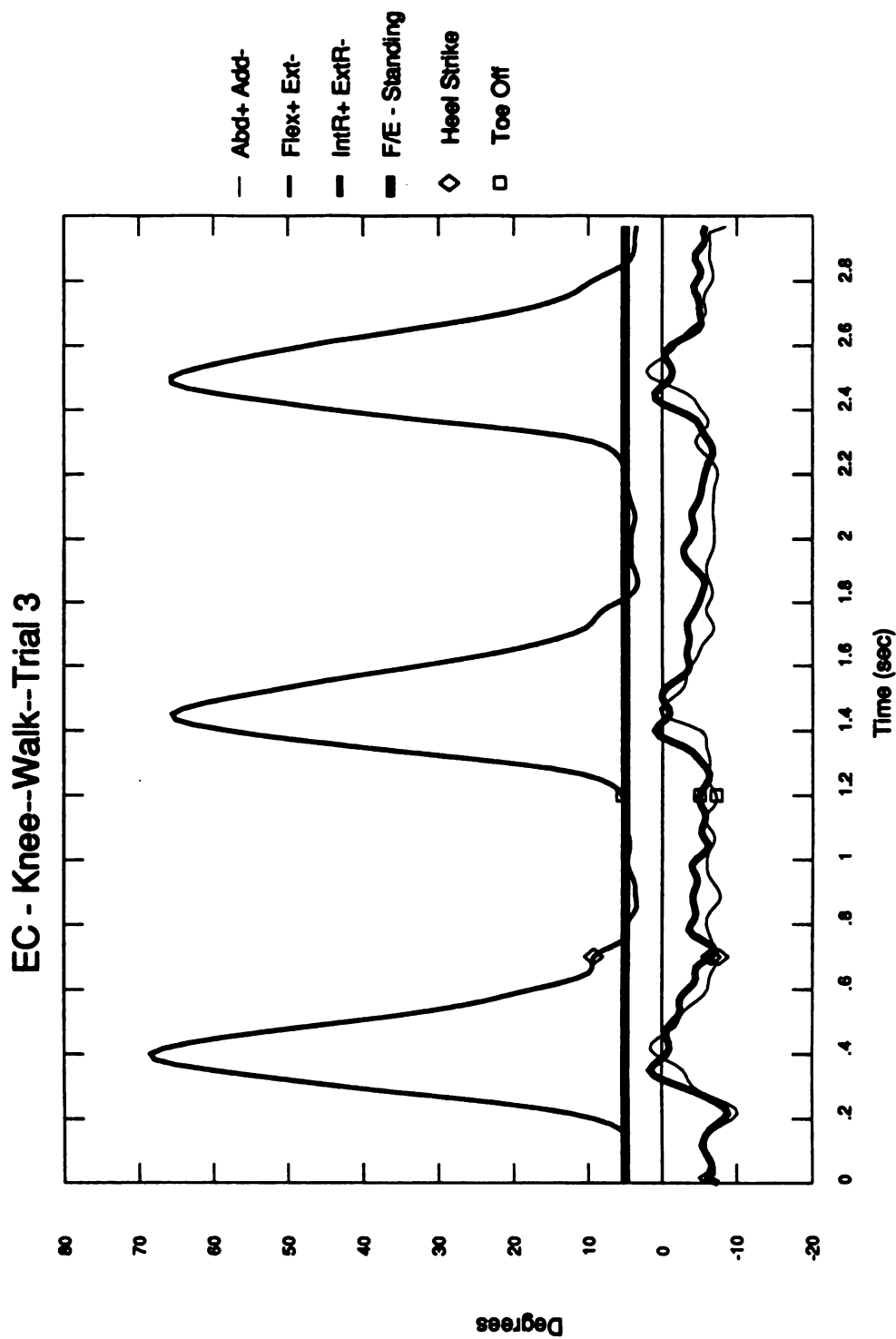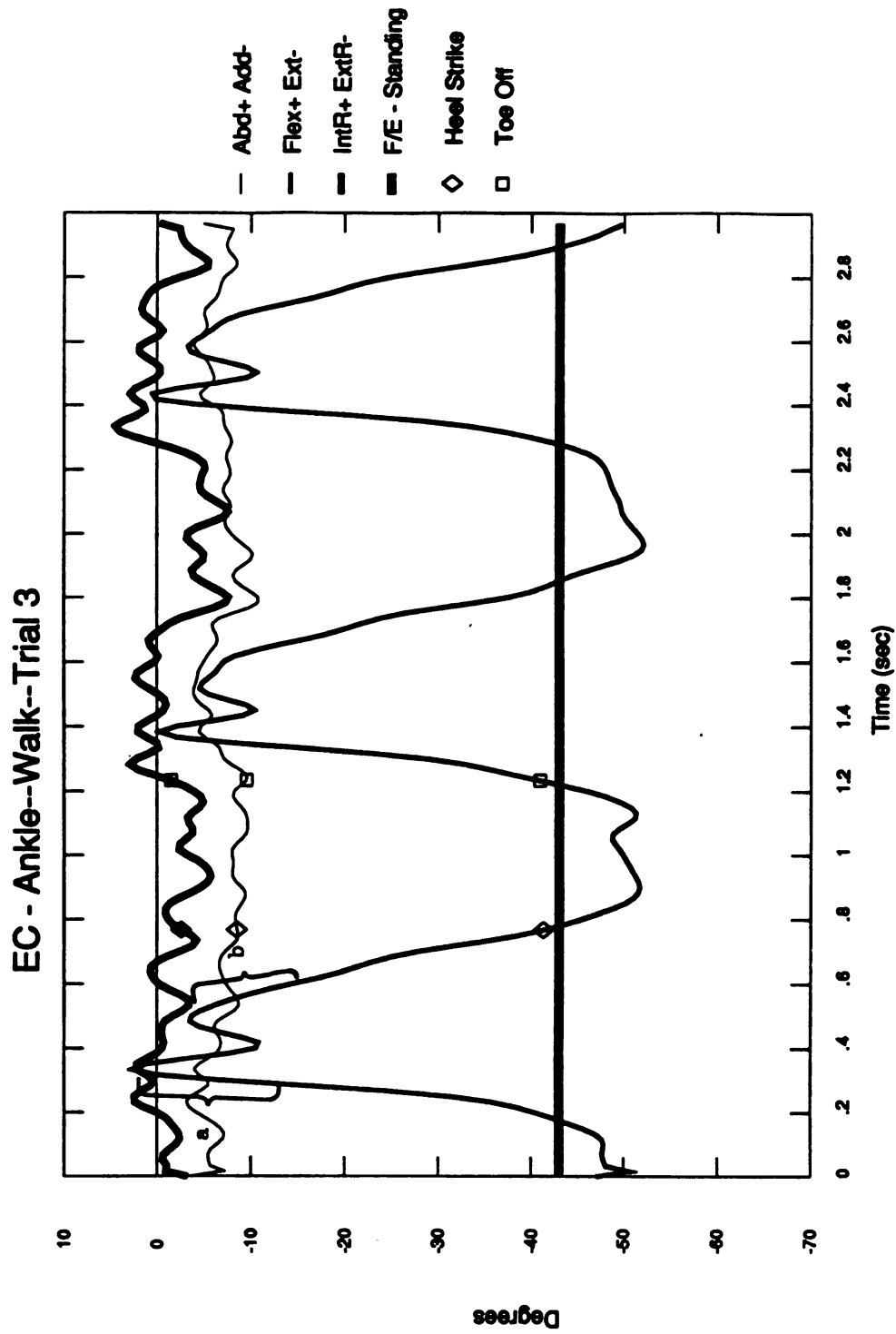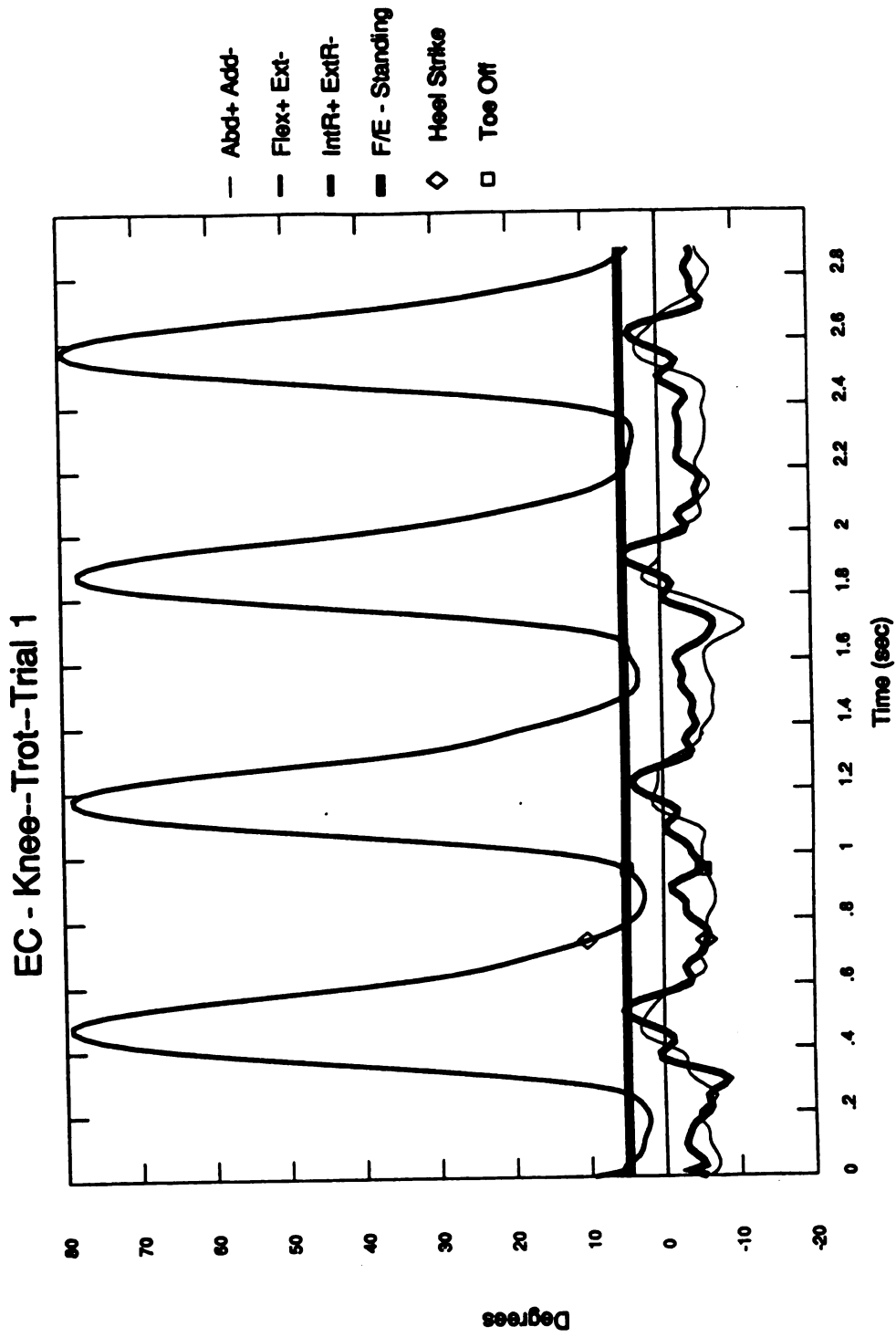
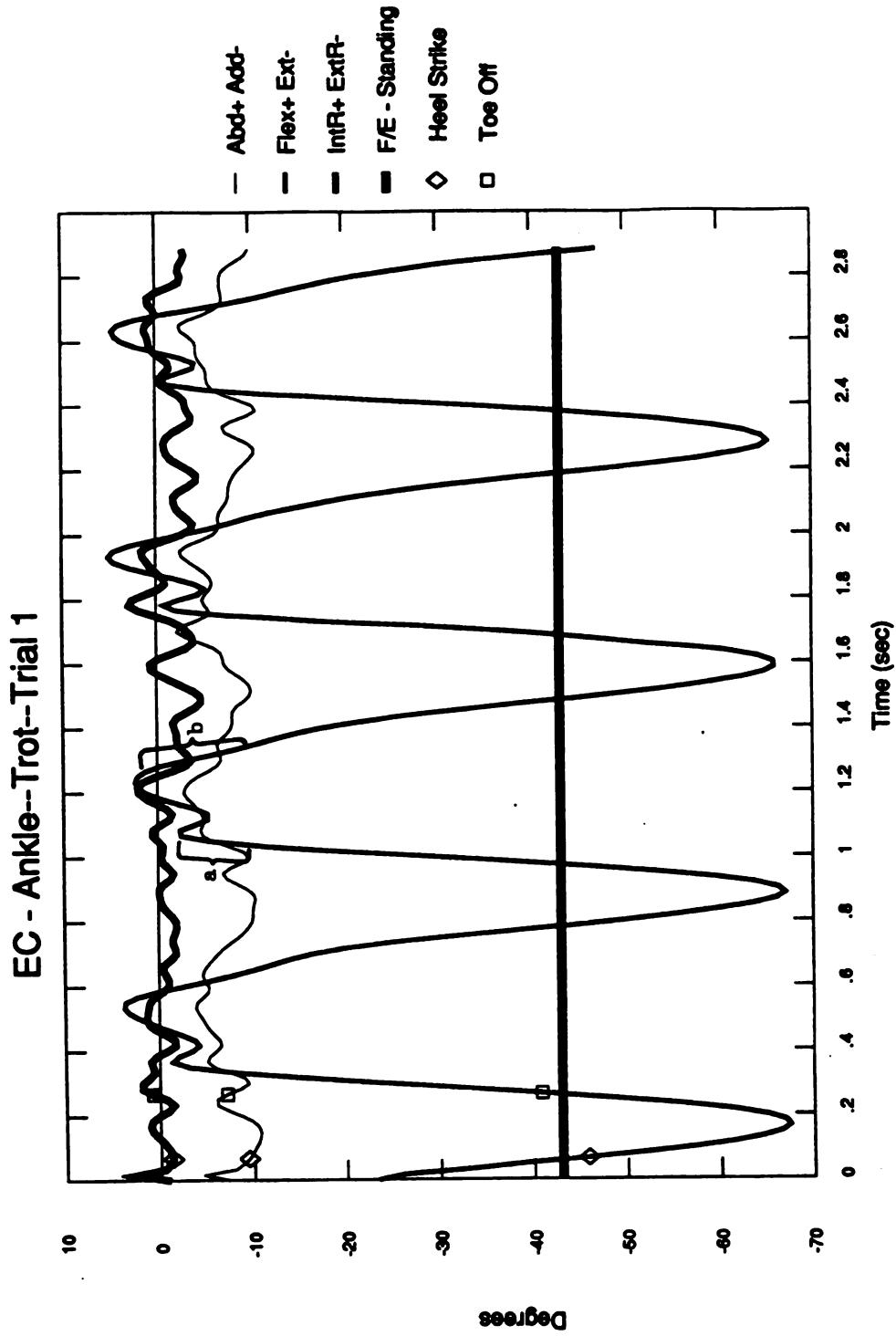Figure 25. Kinematics for the knee joint. See Figures 14 and 16 for further explanation of the legend.

Figure 26. Kinematics for the ankle joint. See Figures 14 and 17 for further explanation of the legend.

Since the ankle was extended even while standing, most of the flexion/extension curve occurred on a negative scale. The ankle sinks considerably during stance phase for shock absorption; consequently, there was a greater continued drop between hoof strike and toe off than what was observed in the knee.

Differences in stance phase and swing phase timings were nearly identical to those observed in the knee. Ranges of motion for the ankle at the walk were approximately 55° flexion/extension and approximately 70° flexion/extension at the trot. Less abduction/adduction took place in subject BS's ankle than occurred in her knee. Unlike the knee, maximum internal rotation in the ankle occurred at approximately midstance during the trot.

The most striking difference when looking at subject EC's ankle graphs (Figures 24 and 26) is that at the walk, peak "a" is larger than peak "b." This differs from this same subject's trotting files, as well as subject BS's walk and trot. Again, the walk graphs were checked and rechecked to be sure this was not an error in analysis. Each check showed the same position of the peaks. With only two subjects, it is impossible to say which subject more closely represents "normal." Since neither subject demonstrated pathological movement, perhaps both are "normal," though one may be more nearly "ideal" than the other.

Flexion/extension ranges of motion for subject EC's ankle were approximately 52° at the walk and 65° at the trot. There

was less difference in scale between peaks "a" and "b" for subject EC's trot than had been observed for subject BS.

Ankle graphs for each condition and each subject were easily identifiable without looking at labels. Knee graphs were somewhat less distinct in their differences between the two subjects, though walk and trot were easily differentiated.

Cross plots, or angle-angle diagrams, of knee against ankle flexion/extension were also plotted (Figures 27-30). The graphs depict approximately three gait cycles for the walk and approximately four gait cycles for the trot. Motion on the plots proceeds in a counter-clockwise direction, and the condensed area in the lower left of each plot represents stance phases. Plots both stretched and narrowed when going from the walk to the trot.

Cross plots probably have the most potential usefulness when analyzing pathologies or documenting interactions. For example, the range of motion of horses with osteoarthritis could be compared before and after administering an anti-inflammatory drug. Also, it has been noted in human studies (Soutas-Little, 1991) that often a pathology in one part of the limb will cause compensatory actions in another part of the limb or in the opposite limb. These interactions are more quickly analyzed using a cross plot than by analyzing the entire set of data.

Figure 27. Cross plot of knee against ankle flexion/
extension. The direction of motion is counter-clockwise.
This plot is for Subject BS while walking.

Figure 28. Cross plot of knee against ankle flexion/
extension. The direction of motion is counter-clockwise.
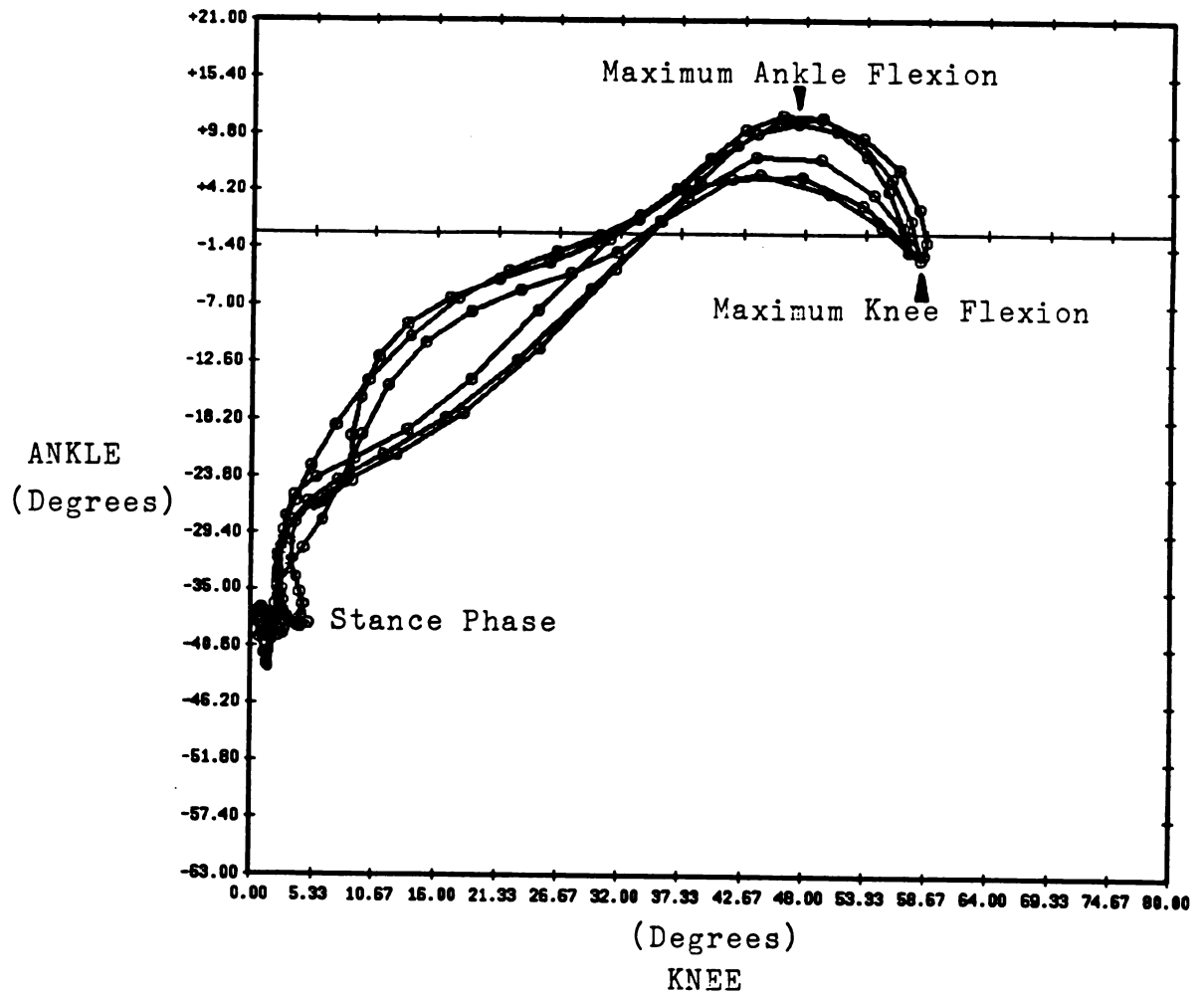This plot is for Subject BS while trotting.

Figure 29. Cross plot of knee against ankle flexion/
extension. The direction of motion is counter-clockwise.
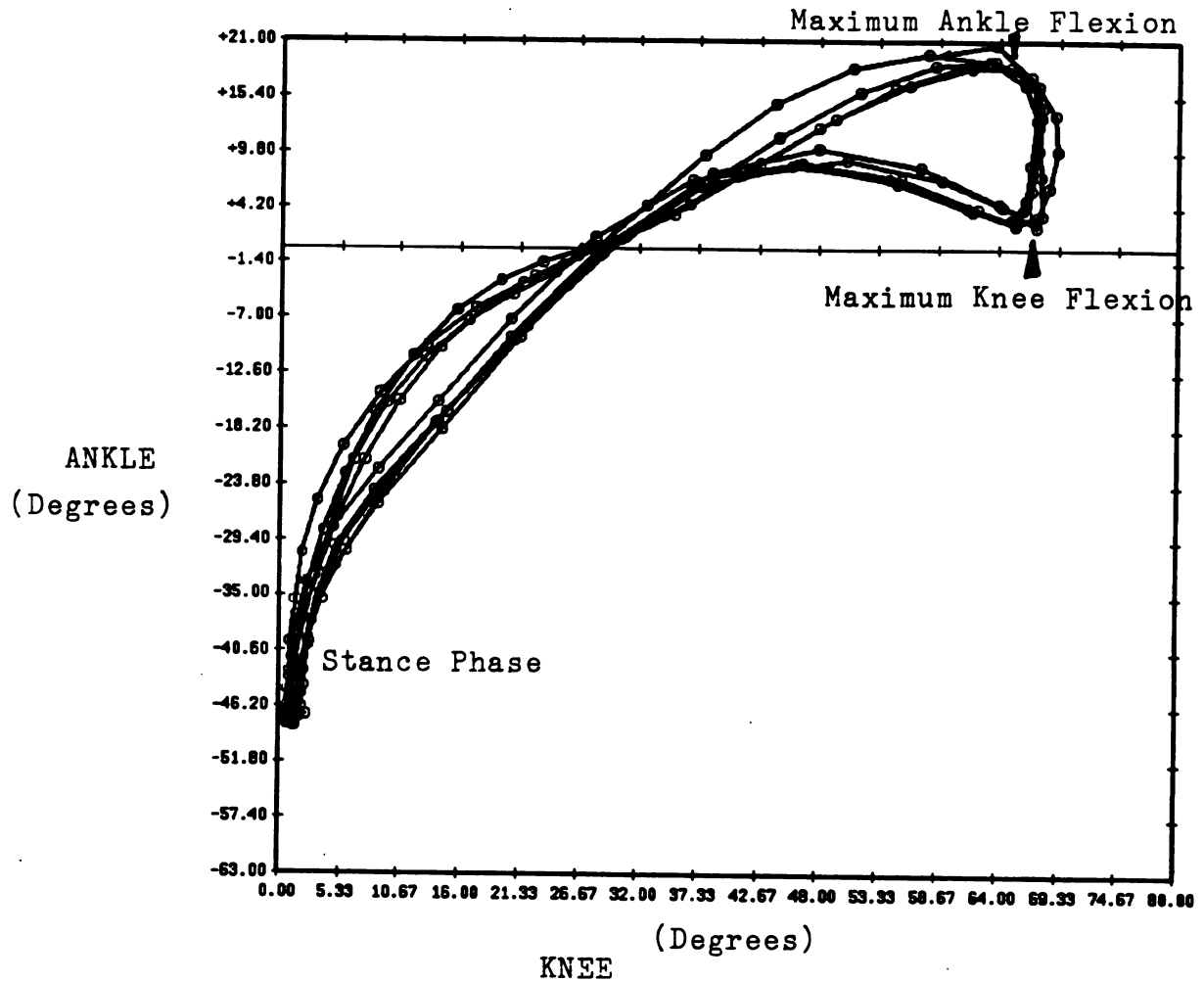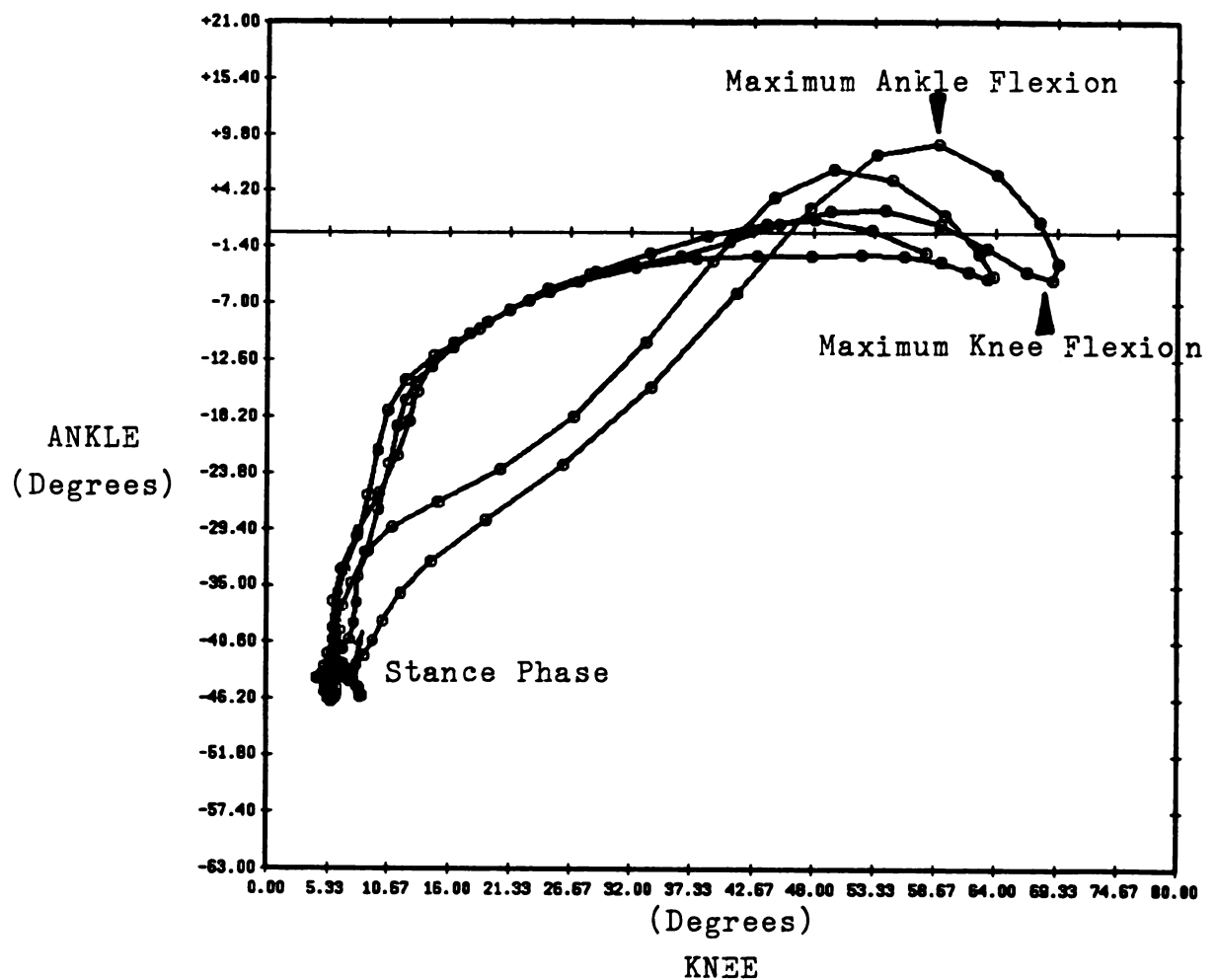This plot is for Subject EC while walking.
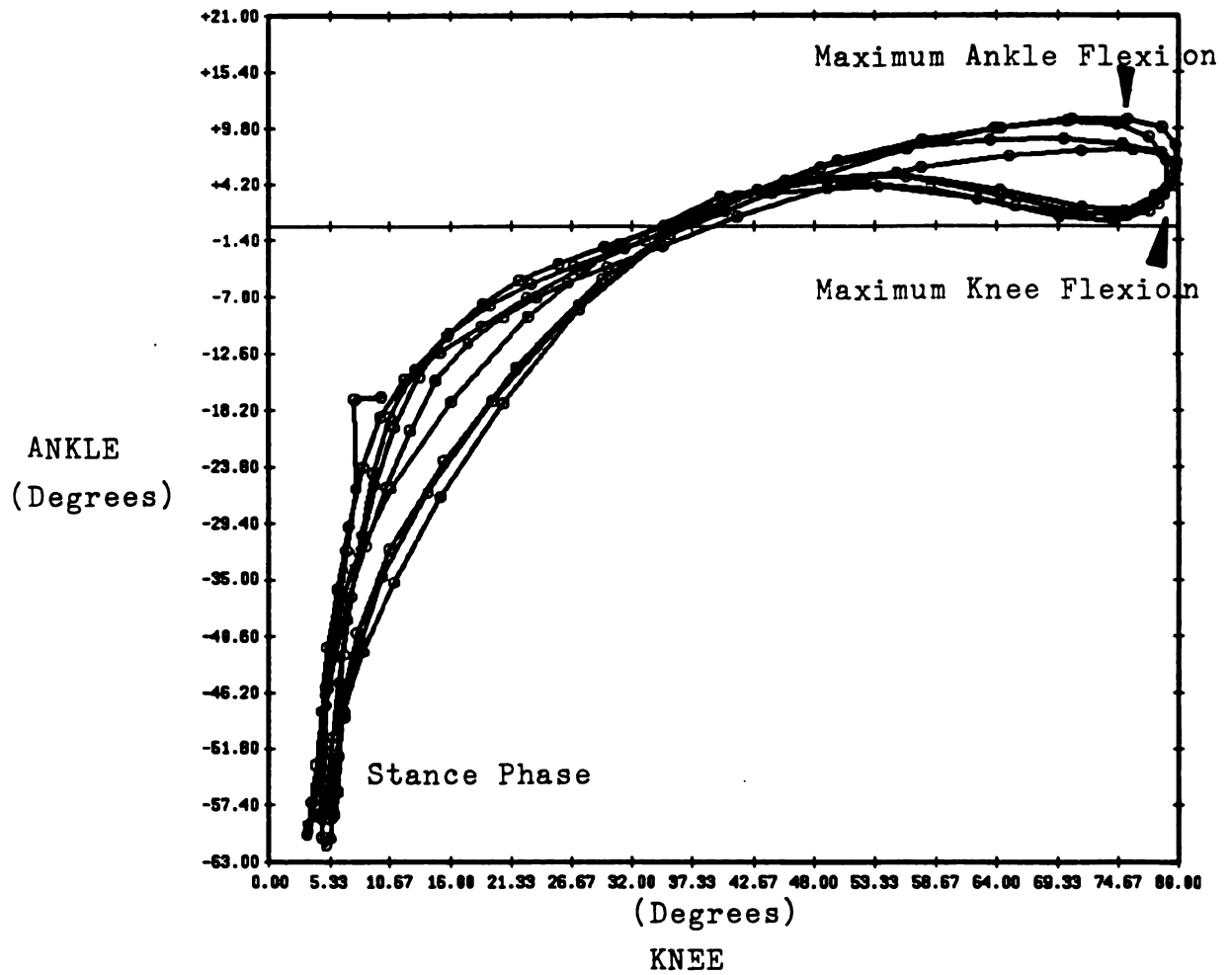
Figure 30. Cross plot of knee against ankle flexion/
extension. The direction of motion is counter-clockwise.
This plot is for Subject EC while trotting.

CONCLUSION

This study describes appropriate methodology for three-dimensional kinematic analysis of the horse's knee and ankle joints. The targeting schemes, camera set-up, calibration area, and joint coordinate analysis programs all contributed to producing reproducible data.

One suggestion for future studies is to have the additional benefit of a force plate or, perhaps, force shoes, to facilitate simultaneous collection of kinetic data. Force data would also enable more accurate identification of hoof strike and toe off. Kinetic data may contribute greatly to more clearly identifying lamenesses, since uneven weightbearing would be detected.

The follow-up step to this study would be to analyze a large enough sample of "normal" (i.e., horses without a noticeable pathology) horses so that baseline data could be accumulated. Since there are most probably breed, age, and training differences among horses, these factors would need to be considered and accounted for. Next, studies of lameness and corrective farrier work (trimming and shoeing) could commence. Studies in these areas would ideally look at all four limbs, at least on some of the subjects, to check for compensatory mechanisms that might be taking place. These studies would hold tremendous potential for the horse industry.

Human biomechanics studies are becoming an acceptable

clinical tool, rather than strictly a research tool. Perhaps in the future, gait analysis will be a routine clinical tool for the evaluation of horses.

APPENDIX

Mathematics involved in calculating frame 1 for the knee of subject BS (see also Figures 1, 9, and 10):

$\overline{F}_1$, $\overline{F}_2$, $\overline{F}_3$, $\overline{C}_4$, $\overline{C}_5$, $\overline{C}_6$, $\overline{P}_7$, $\overline{P}_8$, and $\overline{P}_9$ will all be represented by the actual positional data for each with respect to the calibrated area. Each coordinate is defined by a vector value in the x, y, and z directions. The first three values represent targets 1, 2, and 3 of the forearm; the second three values represent targets 4, 5, and 6 of the cannon; the final three values represent targets 7, 8, and 9 of the pastern.

$$\hat{z}_f = (\overline{F}_1 - \overline{F}_2) \, / \, |\overline{F}_1 - \overline{F}_2|$$

$$= -10.172\hat{i}_x - 1.229\hat{i}_y + 52.216\hat{i}_z \quad \text{(x, y, and z coordinates for target 1 on the forearm)}$$

$$- (-15.934\hat{i}_x - .510\hat{i}_y + 42.925\hat{i}_z) \quad \text{(x, y, and z coordinates for target 2 on the forearm)}$$

$$+ (5.762^2 + .719^2 + 9.291^2)^{1/2}$$ (This is the manner in which vector absolute values are calculated; after the difference between the x, y, and z values of F_1 and F_2 are calculated, these differences are then squared. The values are then added and the square root of the total is taken.)

$$= .526\hat{i}_x - .066\hat{i}_y + .848\hat{i}_z \quad ***$$

$$\hat{y}_f = [\hat{z}_f \times (\overline{F}_3 - \overline{F}_2)] \, / \, |\hat{z}_f \times (\overline{F}_3 - \overline{F}_2)|$$

"x" symbolizes a cross product and is computed in the following manner (using A - F as variables that show how to calculate cross products regardless of the values):

$$\begin{vmatrix} \hat{i}_x & \hat{i}_y & \hat{i}_z \\ A & B & C \\ D & E & F \end{vmatrix} = (BF - CE) \, i_x - (AF - DC) \, i_y + (AE - BD) \, i_z$$

$$-22.010 \; \hat{i}_x - .761 \; \hat{i}_y + 46.953 \; \hat{i}_z \quad \text{(position values for } \overline{F}_3)$$

$$- (-15.936 \; \hat{i}_x - .510 \; \hat{i}_y + 42.925 \; \hat{i}_z) \quad \text{(position values for } \overline{F}_2)$$

$$-6.074 \; \hat{i}_x - .251 \; \hat{i}_y + 4.028 \; \hat{i}_z$$

$$\begin{vmatrix} \hat{1}_x & \hat{1}_y & \hat{1}_z \\ .526 & -.066 & .848 \\ -6.074 & -.251 & 4.028 \end{vmatrix}$$

(see $\hat{z}_f$ from above)

$$= \frac{-.054 \, \hat{1}_x - 7.270 \, \hat{1}_y - .533 \, \hat{1}_z}{(-.054^2 - 7.270^2 - .533^2 \,)^{1/2}}$$

$$= -.007 \, \hat{1}_x - .997 \, \hat{1}_y - .073 \, \hat{1}_z \quad ***$$

$$\hat{x}_f = \hat{y}_f \times \hat{z}_f$$

$$\begin{vmatrix} \hat{1}_x & \hat{1}_y & \hat{1}_z \\ -.007 & -.997 & -.073 \\ .526 & -.066 & .848 \end{vmatrix}$$

($\hat{y}_f$ values from above)

$$= -.850 \, \hat{1}_x - .032 \, \hat{1}_y + .524 \, \hat{1}_z \quad ***$$

($\hat{z}_f$ values from above)

$$\hat{z}_c = (\overline{C}_4 - \overline{C}_5) \, / \, | \, \overline{C}_4 - \overline{C}_5 \, |$$

$$-29.816 \, \hat{1}_x + 4.930 \, \hat{1}_y + 30.469 \, \hat{1}_z \quad \text{(position values for } \overline{C}_4)$$

$$-(-34.042 \, \hat{1}_x + 4.458 \, \hat{1}_y + 20.151 \, \hat{1}_z) \quad \text{(position values for } \overline{C}_5)$$

$$4.226 \, \hat{1}_x + .472 \, \hat{1}_y + 10.318 \, \hat{1}_z \, / \, (4.226^2 + .472^2 + 10.318^2)^{1/2}$$

$$= .379 \, \hat{1}_x + .042 \, \hat{1}_y + .925 \, \hat{1}_z \quad ***$$

$$\hat{y}_c = [\hat{z}_c \times (\overline{C}_5 - \overline{C}_6)] \, / \, | \hat{z}_c \times (\overline{C}_5 - \overline{C}_6) |$$

$$-34.042 \quad + 4.458 \quad + 20.151 \quad \text{(position values for } \overline{C}_5)$$
$$-(-23.736 \quad + 5.321 \quad + 16.666) \quad \text{(position values for } \overline{C}_6)$$

$$-10.306 \, \hat{1}_x - .863 \, \hat{1}_y + 3.485 \, \hat{1}_z$$

$$\begin{vmatrix} \hat{1}_x & \hat{1}_y & \hat{1}_z \\ .379 & .042 & .925 \end{vmatrix}$$

(values for $\hat{z}_c$)

$$\frac{.944 \, \hat{1}_x - 10.854 \, \hat{1}_y + .106 \, \hat{1}_z}{= (.944^2 + 10.854^2 + .106^2)^{1/2}}$$

$$\begin{vmatrix} -10.306 & -.863 & 3.485 \end{vmatrix}$$ (difference between $\tilde{C}_5$ and $\tilde{C}_6$)

$$= .087\hat{i}_x - .996\hat{i}_y + .010\hat{i}_z \quad \text{***}$$

$$\hat{x}_c = \hat{y}_c \times \hat{z}_c$$

$$\begin{vmatrix} \hat{i}_x & \hat{i}_y & \hat{i}_z \\ .087 & -.996 & .010 \\ .379 & .042 & .925 \end{vmatrix}$$

($\hat{y}_c$ values from above)

$= -.921\hat{i}_x -.076\hat{i}_y +.381\hat{i}_z \quad \text{***}$

($\hat{z}_c$ values from above)

$\hat{e}_1$, $\hat{e}_2$, and $\hat{e}_3$ represent the Euler angles of motion (see Figure 9).

$$\hat{e}_2 = \hat{y}_f$$

$$\hat{e}_3 = \hat{z}_c$$

$$\hat{e}_1 = (\hat{e}_2 \times \hat{e}_3) \, / \, |\hat{e}_2 \times \hat{e}_3|$$

$$\begin{vmatrix} \hat{i}_x & \hat{i}_y & \hat{i}_z \\ -.007 & -.997 & -.073 \\ .379 & .042 & .925 \end{vmatrix}$$

(values for $\hat{e}_2 = \hat{y}_f$)

$$= \frac{-.925\hat{i}_x -.022\hat{i}_y +.379\hat{i}_z}{(.925^2 +.022^2 +.379^2)^{1/2}}$$

(values for $\hat{e}_3 = \hat{z}_c$)

$$= -.925\hat{i}_x -.021\hat{i}_y +.380\hat{i}_z \quad \text{***}$$

internal/external rotation = $\sin^{-1}$ ($\hat{e}_1 \cdot \hat{y}_c$) (For dot products, represented by " • ", only the values are important, not the direction)

$$(-.925 \, -.021 \, +.380) \cdot (.087 \, -.996 \, +.010)$$
(values for $\hat{e}_1$)   (values for $\hat{y}_c$)

-.080 (this is the first values multiplied together)
+.021 (this is the second values multiplied together)
+.004 (this is the third values multiplied together)

$$\overline{-.055}$$

$$= \sin^{-1} -.055$$

$$= -3.16^{\circ} \quad \text{***}$$

flexion/extension $= -\sin^{-1} (\hat{e}_1 \cdot \hat{z}_f)$

$(-.925 \ -.022 \ +.379) \cdot (.526 \ -.066 \ +.848)$
(values for $\hat{e}_1$)   (values for $\hat{z}_f$)

$-.487 \ +.001 \ +.321 = -.165$

$= -\sin^{-1} \ -.165$

$= 9.49^{\circ}$ ***

abduction/adduction $= \sin^{-1} (\hat{e}_2 \cdot \hat{e}_3)$

$(-.007 \ -.997 \ -.073) \cdot (.379 \ +.042 \ +.925)$
(values for $\hat{e}_2$)   (values for $\hat{e}_3$)

$-.003 \ -.042 \ -.068 = -.113$

$= \sin^{-1} \ -.113$

$= -6.488^{\circ}$ ***

Mathematics involved in calculating frame 1 of the ankle for subject BS:

$\hat{z}_c = .379\hat{i}_x \ +.042\hat{i}_y \ +.925\hat{i}_z$ (see knee calculations)

$\hat{y}_c = .087\hat{i}_x \ -.996\hat{i}_y \ +.010\hat{i}_z$ (see knee calculations)

$\hat{x}_c = -.921\hat{i}_x \ -.076\hat{i}_y \ +.381\hat{i}_z$ (see knee calculations)

$\hat{z}_p = (\bar{P}_7 \ -\bar{P}_8) \ / \ |\bar{P}_7 \ -\bar{P}_8|$ (x, y, and z coordinates from targets 7 and 8 on the pastern)

$\begin{array}{rrr} -32.647 & -.614 & +11.218 \\ \underline{+36.826} & \underline{+1.915} & \underline{-6.776} \end{array}$

$4.179\hat{i}_x \ +1.301\hat{i}_y \ +4.442\hat{i}_z$

$\dfrac{4.179\hat{i}_x \ +1.301\hat{i}_y \ +4.442\hat{i}_z}{(4.179^2 \ +1.301^2 \ +4.442^2)^{1/2}} = .670\hat{i}_x \ +.209\hat{i}_y \ +.712\hat{i}_z$ **

$\hat{y}_p = [\hat{z}_p \ x \ (\bar{P}_8 \ -\bar{P}_9)] \ / \ |\hat{z}_p \ x \ (\bar{P}_8 \ - \ \bar{P}_9)|$

$\begin{array}{rrr} -36.826 & -1.915 & +6.776 \\ \underline{+32.593} & \underline{+1.200} & \underline{-3.092} \end{array}$ (position values for $\bar{P}_8$)
(position values for $\bar{P}_9$)

$$-4.233\hat{i}_x \quad -.715\hat{i}_y \quad +3.684\hat{i}_z$$

$$\begin{vmatrix} \hat{i}_x & \hat{i}_y & \hat{i}_z \\ .670 & .209 & .712 \\ & & \\ -4.233 & -.750 & 3.684 \end{vmatrix}$$

(values for $\hat{z}_p$)

$$= \frac{1.279\hat{i}_x \ -5.481\hat{i}_y \ +.406\hat{i}_z}{(1.279^2 +5.481^2 +.406^2)^{1/2}}$$

$$= .277\hat{i}_x -.971\hat{i}_y +.072\hat{i}_z \quad **$$

$$\hat{x}_p = \hat{y}_p \times \hat{z}_p$$

$$\begin{vmatrix} \hat{i}_x & \hat{i}_y & \hat{i}_z \\ .227 & -.971 & .072 \\ & & \\ .670 & .209 & .712 \end{vmatrix}$$

(values for $\hat{y}_p$)

$$= (-.691 -.015)\hat{i}_x - (.162 -.048)\hat{i}_y + (.047 + .651)\hat{i}_z$$

(values for $\hat{z}_p$)

$$= -.706\hat{i}_x -.114\hat{i}_y +.698\hat{i}_z \quad **$$

$\hat{e}_1'$, $\hat{e}_2'$, $\hat{e}_3'$ represent the Euler angles of motion (see Figure 10).

$$\hat{e}_2' = \hat{y}_c = .087\hat{i}_x -.996\hat{i}_y +.010\hat{i}_z$$

$$\hat{e}_3' = \hat{z}_p = .670\hat{i}_x +.209\hat{i}_y +.712\hat{i}_z$$

$$\hat{e}_1' = (\hat{e}_2 \times \hat{e}_3) / |\hat{e}_2' \times \hat{e}_3'|$$

$$\begin{vmatrix} \hat{i}_x & \hat{i}_y & \hat{i}_z \\ .087 & -.996 & .010 \\ & & \\ .670 & .209 & .712 \end{vmatrix}$$

(values for $\hat{e}_2$)

$$= \frac{-.711\hat{i}_x -.055\hat{i}_y +.685\hat{i}_z}{(.711^2 +.055^2 +.685^2)^{1/2}}$$

(values for $\hat{e}_3$)

$$= -.719\hat{i}_x -.056\hat{i}_y +.693\hat{i}_z \quad **$$

flexion/extension $= -\sin^{-1} (\hat{e}_1' \cdot \hat{z}_c)$

$$(-.719 -.056 +.693) \cdot (.379 +.082 +.925)$$

$$-.273 \ -.002 \ +.641$$

$$= -\sin^{-1} .366$$

$$= -21.47^\circ \ **$$

abduction/adduction $= \sin^{-1} (\hat{e}_2{}' \cdot \hat{e}_3{}')$

$$(.087 \ -.996 \ +.010) \cdot (.670 \ +.209 \ +.712)$$

$$.058 \ -.208 \ +.007$$

$$= \sin^{-1} -.143$$

$$= -8.22^\circ \ **$$

internal/external rotation $= \sin^{-1} (\hat{e}_1{}' \cdot \hat{y}_p)$

$$(-.719 \ -.056 \ -.693) \cdot (.227 \ -.971 \ +.072)$$

$$-.163 \ +.054 \ +.050$$

$$= \sin^{-1} -.059$$

$$= -3.388^\circ \ **$$

LIST OF REFERENCES

LIST OF REFERENCES

Auer, J.A., Fackelman, G.E., Gingerich, D.A. and Fetter, A.W. 1980. Effect of hyaluronic acid in naturally occurring and experimentally induced osteoarthritis. Am. J. Vet. Res., 41, 568-574.

Barclay, O.R. 1953. Some aspects of the mechanics of mammalian locomotion. J. Exp. Biol., 30, 116-120.

Bartel, D.L., Schryver, H.F., Lowe, J.E. and Parker, R.A. 1978. Locomotion in the horse: A procedure for computing the internal forces in the digit. Am. J. Vet. Res., 39, 1721-1727.

Bayer, A. 1973. Bewegungsanalysen an Trabrennpferden mit Hilfe der Ungulographie. <Movement analysis in trotters with the aid of ungulography>. Zentbl. Vet. med. Reihe A, 20, 209-221.

Benke, G. 1934. Vizsgálatok különbözö fajtajellegü és hasznosit ás lovak súlypontjának meghatározasáról és v áltozásaról. <Contribution to the determination of changes in center of gravity of horses>. Thesis, Budapest, 30 pp.

Björck, G. 1958. Studies on the draught forces of horses: Development of a method using strain guages for measuring forces between hoof and ground. Acta Agric. Scand., 8, Suppl. 4.

Borod, J.C., Caron, H.S. and Koff, E. 1984. Left-handers and right-handers compared on performance and preference measures of lateral dominance. Br. J. Psych., 75, 177-186.

Cheney, J.A., Shen, C.K. and Wheat, J.D. 1973. Relationship of racetrack ' surface to lameness in the Thoroughbred racehorse. Am. J. Vet. Res., 34, 1285-1289.

Chieffi, A. and de Mello, L.H. 1939. Contribuição para o estudo da localizacão do centro de gravidade no corpo dos animais domésticos e dos fatores que produzem seu deslocamento temporário ou permanente. <Contribution to the study of location of the center of gravity in domestic animals and the factors promoting temporary or permanent dislocation>. Rev. Fac. Med. Vet. S. Paulo, 1,

97-154.

Clayton, H. 1988. What makes a cutting horse great. Equus,
143, 46-50.

d'Enrödy, A.L. 1967. Give Your Horse a Chance. J.A. Allen &
Co., London.

Dalin, G., Drevemo, S., Fredricson, I., Jonsson, K. and
Nilsson, G. 1973. Ergonomic aspects of locomotor
asymmetry in Standardbred horses trotting through turns.
Acta Vet. Scand., 38, Suppl. 44, 111-139.

Dalin, G. and Jeffcott, L.B. 1985. Locomotion and gait
analysis. Vet. Clin. North Am. Equine Pract., 1(3), 549-
572.

Deuel, N.R. and Lawrence L.M. 1985a. Effects of velocity on
gallop limb contact variables. Proc. 9th Equine Nutr. and
Physiol. Symp., 254-259.

Deuel, N.R. and Lawrence, L.M. 1985b. Bilateral asymmetry in
gallop motion: handedness in horses. Proc. Am. Soc.
Biomech. Mtg., 9, 57-58.

Deuel, N.R. and Lawrence, L.M. 1987. Effects of urging by the
rider on equine gallop stride limb contacts. Proc. 10th
Equine Nutr. and Physiol. Symp., 487-492.

Deuel, N.R. and Lawrence, L.M. 1988. Neck and shoulder motion
of the gallop stride. J. Eq. Vet. Sci., 8(3), 243-248.

Deuel, N.R. and Park, J. 1989. Temporal characteristics of the
extended trot of superior Olympic dressage horses. Proc.
11th Equine Nutr. and Physiol. Symp., 17-19.

Drevemo, S., Dalin, G., Fredricson, I. and Hjertén, G. 1980a.
Equine locomotion: 1. The analysis of linear and temporal
stride characteristics of trotting Standardbreds. Equine
Vet. J., 12(2), 60-65.

Drevemo, S., Fredricson, I., Dalin, G. and Björne, K. 1980b.
Equine locomotion: 2. The analysis of coordination
between limbs of trotting Standardbreds. Equine Vet. J.,
12(2), 66-70.

Drevemo, S., Dalin, G., Fredricson, I. and Bjorne, K. 1980c.
Equine locomotion. 3. The reproducibility of gait in
Standardbred trotters. Equine Vet. J., 12(2), 71-73.

Dusek, J., Ehrlein, H.J., van Engelhardt, W. and Hörnicke, H.
1970. Beziehungen zwischen Trittlänge, Trittfrequenz und
Geschwindigkeit bei Pferden. <Relationships between
stride length, stride frequency and velocity in horses>.

Z. Tierärztl. Zücht. Biol., 87, 177-188.

Frederick, Jr., F.H. and Henderson, J.M 1970. Impact force measurement using preloaded transducers. Am. J. Vet. Res., 31, 2279-2283.

Fredricson, I. and Drevemo, S. 1971. A new method of investigating equine locomotion. Equine Vet. J., 3, 137-140.

Fredricson, I., Drevemo, S., Moen, K., Dandanell, R. and Andersson, B. 1972. A method of three-dimensional analysis of kinematics and co-ordination of equine extremity joints. Acta Vet. Scand., 13, Suppl. 37, 1-44.

Fredricson, I. and Drevemo, S. 1972. Variations of resultant joint co-ordination patterns in fast-moving Standardbreds. Acta Vet. Scand., 13, Suppl. 37, 65-92.

Fredricson, I. and Nilsson, G. 1974. Asymmetry of movement caused by inadequate camber of racetracks. Proc. 12th Nordic Vet. Congr., pp. 906-924.

Fredricson, I., Daling, G., Drevemo, S., Hjerten, G., Nilsson, G. and Alm, L. 1975a. Ergonomic aspects of poor racetrack design. Equine Vet. J., 7(2), 63-65.

Fredricson, I., Dalin, G., Drevemo, S. and Hjerten, G. 1975b. A biotechnical approach to the geometric design of racetracks. Equine Vet. J., 7(2), 91-96.

Geary, Jr., J.E. 1975. The dynamics of the equine foreleg. Masters of Mech. Aerosp. Engineering, Univ. of Delaware.

Gingerich, D.A. and Newcomb, K.M. 1979. Biomechanics of lameness. J. Equine Med. Surg., 3(6), 252-252.

Gingerich D.A., Auer, J.A. and Fackelman, G.E. 1981. Effect of exogenous hyaluronic acid on joint function in experimentally induced equine osteoarthritis: dosage titration studies. Res. Vet. Sci. 30, 192-197.

Goubaux, A. and Barrier G. 1884. De l'Exterieur du Cheval. <The exterior of the horse>. J.B. Lippincott Co., Philadelphia.

Gray, J. 1944. Studies on the mechanics of the tetrapod skeleton. J. Exp. Biol., 20, 88-116.

Gray, J. 1968. Animal Locomotion. Weidenfeld & Nicholson, London.

Grood, E.S. and Suntay, W.J. 1983. A joint coordinate system for the clinical description of three-dimensional

motions. J. Biomech. Eng. Trans. ASME, 105, 136-144.

Hayes, M.H. 1893. Points of the Horse. (Republished 7th revised edn. 1969), Arco Publishing Co., N.Y., 541 pp.

Hékimian, E. 1970. Réflexions sur la locomotion du cheval: l'équilibre dynamique. <Thoughts on the locomotion of the horse: dynamic equilibrium>. Mammalia, 34, 118-135.

Herbert, K.S. 1988. A leg up. Blood Horse, April 9, 2092-2101.

Howell, A.B. 1944. Speed in Animals. Hafner Publishing Co., N.Y.

Ivers, T. 1985. Equine Sportsmedicine Review. 224 pp.

Kilby, E. 1988. New angles on hoof angles. Equus, 127, 67-123.

Krüger, W. 1940. Die Fortbewegung des Pferdes. <The locomotion of the horse>. Tierärztl. Fundsch., 46, 8.

Krüger, W. 1941. Ueber das Verhalten des Schwerpunktes bei normalen Fortbewegung des Pferdes. <The center of gravity in normal locomotion of horses>. Tierärztl. Rundsch., 13, 162-166.

Leach, D.H. and Crawford, W.H. 1983. Guidelines for the future of equine locomotion research. Equine Vet. J. 15, 103-110.

Leach, D.H. and Dagg, A.I. 1983a. A review of research on equine locomotion and biomechanics. Equine Vet. J., 15, 93-102.

Leach, D.H. and Dagg, A.I. 1983b. Evolution of equine locomotion research. Equine Vet. J., 15, 87-92.

Leach, D.H. 1987. Noninvasive technology for assessment of equine locomotion. The Comp. Cont. Educ. for the Pract. Veterinarian, 9(11), 1124-1135.

Leach, D.H., Sprigings, E.J. and Laverty, W.H. 1987. A multivariate statistical analysis of stride timing measurements of nonfatigued racing Thoroughbreds. Am. J. Vet. Res., 48(5), 880-888.

Lenoble du Tei J.J. 1877a. Étude sur la locomotion de l'homme et des quadrupèdes en général. <Study of the locomotion of man and the quadrupeds in general>. Cited by A. Goubaux and C. Barrier 1904 in The Exterior of the Horse. 2nd edn., J.B. Lippincott, Philadelphia.

Lenoble du Teil, J.J. 1877b. Locomotion Quadrupède Études sur

le Cheval. <Quadrupedal locomotion studies on the horse>.
J. Haras.

Lenoble du Teil, J.J. 1893. Les allures du Cheval dévoileés
par la methode expérimentale - conduite du cheval
simplifieé. <The gait of the horse revealed by the
experimental method - taken of the simplified horse>.
Berger Levrault, Paris, 223 pp.

Mackay-Smith, M.P. 1977. Report - committed to study the
prevention of lameness in racehorses. Report to the
American Assn. of Equine Practitioners Executive Board,
Am. Assn. equine Pract. Newsletter, 1, 33-38.

Manter, J.T. 1938. Dynamics of quadrupedal walking. J. Exp.
Biol., 15, 522-540.

May, S.A. and Wyn-Jones, G. 1987. Identification of hindleg
lameness. Equine Vet. J., 19(3), 185-188.

Merkens, H.W., Schamhardt, H.C., Hartman, W. and Kersjes, A.W.
1988. The use of H(orse) INDEX: A method of analysing the
ground reaction force patterns of lame and normal gaited
horses at the walk. Equine Vet. J., 20(1), 29-36.

Merkens, H.W.and Schamhardt, H.C. 1988. Distribution of
ground reaction forces of the concurrently loaded limbs
of the Dutch Warmblood horse at the normal walk. Equine
Vet. J., 20(3), 209-213.

Muybridge, E. 1899. Animals in Motion. An electro-photographic
investigation of consecutive phases of animal progressive
movements. Chapman and Hall, Ltd. London, 264 pp.

Niki, Y., Ueda, Y., Yoshida, K. and Masumitsu, H. 1982. A
force plate study in equine biomechanics. 2. The vertical
and fore-aft components of floor reaction forces and
motion of equine limbs at walk and trot. Bull. Equine
Res. Inst., 19, 1-17.

Peloso, J.G., Stick, J.A., Soutas-Little, R.W., Caron, J.P.
and DeCamp, C.E. 1991. Computer-assisted three
dimensional gait analysis of amphotericin-induced equine
carpal lameness. Vet. Surg. 20(5), 344.

Pratt, Jr., G.W. and O'Connor, Jr., J.T. 1976. Force plate
studies of equine biomechanics. Am. J. Vet. Res., 37,
1251-1255.

Pratt, Jr., G.W. and O'Connor, Jr., J.T. 1978. A relationship
between gait and breakdown in the horse. Am. J. Vet.
Res., 39, 249-253.

Preuschoft, H. 1989. The external forces and internal stresses

in the feet of dressage and jumping horses. Z. S-äugetierkunde, 54, 172-190.

Quddus, M.A., Kingsbury, H.B. and Rooney, J.R. 1978. A force and motion study of the foreleg of a Standardbred trotter. J. Equine Med. Surgery., 2, 233-242.

Ratzlaff, M.H., Grant, B.D. and Adrian, M. 1982. Quantitative evaluation of equine carpal lamenesses. J. Equine Vet. Sci., 2, 78-88.

Ratzlaff, M., Frame, J., Miller, L., Kimbrell, J. and Grant, B. 1985. A new method for repetitive measurements of locomotor forces from galloping horses. Proc. 9th Equine Nutr. Physiol. Symp., pp. 260-265.

Rettenmaier, L. 1950 Das Verhalten einiger physiologischer Komponenten im Verlauf der gestaffelten Dauerzug - und Geschwindigkeitsprüfung bei Hengsten. <The behavior of some physiological components on the course of a staggered, constant pull - and the velocity examination of stallions>. Dissertation, Giessen.

Rooney, J.R. 1984a. The angulation of the forefoot and pastern of the horse. J. Equine Vet. Sci., 4(3), 138-143.

Rooney, J.R. 1984b. Preliminary observations on stride length and frequency in relation to velocity of horses. J. Equine Vet. Sci., 4(1), 33-34.

Rooney, J.R. 1986. A model for horse movement. J. Equine Vet. Sci. 6(1), 30-34.

Rybicki, E.F., Mills, E.J., Turner, A.S. and Simonen, F.A. 1977. In vivo and analytical studies of forces and moments in equine long bones. J. Biomech., 10, 701-705.

Schryver, H.F., Bartel, D.L., Langrana, N. and Lowe, J.E. 1978. Locomotion in the horse: Kinematics and external and internal forces in the normal equine digit in the walk and trot. Am. J. Vet. Res., 39, 1728-1733.

Smith, J.A. and Ross, W.D. 1910. The works of Aristotle, Vol. IV, Historia Animalium. Translated by D'Arcy Wentworth Thompson. Clarendon Press, Oxford.

Soutas-Little R.W., Beavis, C.G., Verstraete, M.C. and Markus, T.L. 1987. Analysis of foot motion during running using a joint coordinate system. Med. Sci. Sports. Ex., 19, 185-293.

Soutas-Little, R.W. 1991. Personal communication. Michigan State University Biomechanics Evaluation Laboratory, East Lansing, MI.

Sprigings, E. and Leach, D.H. 1986. Standardised technique for determining the centre of gravity of body and limb segments of horses. Equine Vet. J., 18(1), 43-49.

Steiss, J.E., Yuill, G.T., White, N.A. and Bowen, J.M. 1982. Modifications of a force plate system for equine gait analysis. Am. J. Vet. Res., 43(3), 538-540.

Ueda, Y., Niki, Y., Yoshida, K. and Masumitsu, H. 1981. Force plate study of equine biomechanics. Floor reaction force of normal walking and trotting horses. Bull. Equine Res. Inst., 18, 28-41.

Ulibarri, V.D. 1984. An introduction to high speed cinematographic procedures and analysis. Kinko's Press, East Lansing, MI.

Ulibarri, V.D., Papsidero, J.A., Soutas-Little, R.W., Verstraete, M.C. and Peltier, R.A. 1987. Gait characteristics in the older adult. Eng. Sci. Preprints, Society of Engineering Science, 1-10.

Walton, J.S. 1981. Close range cine-photogrammetry; a generalized technique for quantifying gross human motion. Unpublished doctoral thesis, Pennsylvania State University library, State College, PA.

Wentink, G.H. 1978. An experimental study on the role of the reciprocal tendinous apparatus of the horse at walk. Anat. Embryol., 154, 143-151.